Robust Control for Inter-area Oscillations

Katelynn Atkins Vance

Thesis submitted to the faculty of the Virginia Polytechnic Institute and State University in partial fulfillment of the requirements for the degree of

Master of Science

in

Electrical Engineering

Committee Members

James S. Thorp (Chairman)

Virgilio A. Centeno

Jaime De La Ree Lopez

December 6, 2011

Blacksburg, Virginia

Keywords: Inter-area Oscillations, Linear Matrix Inequality (LMI) Control, Polytopic Model, Adaptive Selection, Convex Combination

Robust Control for Inter-area Oscillations

Katelynn Atkins Vance

Abstract

In order to reduce the detrimental effects of inter-area oscillations on system stability, it is possible to use Linear Matrix Inequalities (LMIs) to design a multi-objective state feedback. The LMI optimization finds a control law that stabilizes several contingencies simultaneously using a polytopic model of the system. However, the number of cases to be considered is limited by computational complexity which increases the chances of infeasibility. In order to circumvent this problem, this Thesis presents a method for solving multiple polytopic problems having a common base case. The proposed algorithm determines the necessary polytopic control for a particular contingency and classifies the data as belonging to that polytopic domain. The technique has been tested on an 8-machine, 13 bus, system and has been found to give satisfactory results.

To My Family: Leonard, Toni, Tyler Vance, and Ida Testa

Acknowledgements

It is difficult to explain the process through which an adviser and a graduate student complete a research objective. The question and answer cycle seems never ending, and maybe it is. For the patience and guidance required to support me in pursuing my thesis, I am extremely thankful to Dr. James Thorp. Without his expertise, intuition, and white pages of scratch paper, this thesis would not have been possible.

Additionally, I want to thank Dr. Virgilio Centeno and Dr. Jaime De La Ree Lopez for their contributions throughout this thesis. Their advice has been helpful and motivating.

The students in the Center for Power & Energy provided immeasurable support. They have given me the opportunity to work in an exceptional environment with intelligent and motivated students for which I could not be more thankful. In particular, I would like to thank Anamitra Pal for his willingness to discuss any type of problem. Additionally, I want to thank Shravan Garlapati and Santhosh Sambamoorthy for aiding in my initial studies of this topic.

I would like to extend my gratitude to my parents and brother who contributed immensely to my success in this program. It is only with their help and encouragement that I could have achieved this goal. Additionally, I would like to thank my extended family for further supporting me in my academic pursuits.

Table of Contents

List of Figures

List of Tables

Chapter 1 – Introduction

Chances are this thesis will be read in its electronic version far more than in its paper version. This is significant because it requires the reader to have a computer, powered by electricity, to read it. However, this is not unique to my thesis. Many, if not all, books, journals, magazines, newspapers, and other formerly non-electricity dependent information sources have been made available to those with access to electricity. The ease with which millions of people can access information in an electronic form is just one of many reasons for the increase in electricity consumption. Electricity accounts for over one third of the power consumption of the United States each year [1]. The resulting economic and cultural reliance on electricity make it invaluable to many societies all over the world.

The power grid is a critical part of the U.S. infrastructure given its economic impact. In 2010, the power industry was a $369 billion dollar per year business in the United State alone. Without power, most businesses cannot operate, employees cannot work, and the daily routine, which has become increasingly dependent on electricity, grinds to a halt. The most extreme, recent example of this in the U.S.A. is the 2003 Northeastern Blackout. Billions of dollars were lost when most of the northeast of the United States and parts of Canada lost power.

The implications of a massive power failure are evident in the history of the power system's development. From the 1890's, alternating current (AC) evolved as the dominant mode of electric power. The first U.S. AC systems operated at various frequencies, until 60 Hz was chosen as the national standard. Initially, electric power companies developed as isolated private companies serving a defined geographic area. Over time, they began to interconnect, improving reliability and economy. Electric cooperatives were created in the 1930s, bringing power to rural areas too remote to be reached by commercial private power companies. The downside of interconnections is that regional blackouts can occur due to stress on the interconnecting boundaries.

For the first seven decades of the 1900s, the power demand grew at a rate averaging 7% per year. The demand growth rate has dropped significantly over the past four decades, languishing in the

2-3% range. Although new generators continuously come online, the grid has not been maintained at remotely the same pace. This has resulted in major stability and reliability issues.

The industry is now moving toward a horizontal structure where generating companies, transmission companies, and distribution companies, all act as separate business entities. In 1996, the Federal Energy Regulatory Commission (FERC) issued a ruling requiring open access of all generators to the grid. Independent power producers and co-generators now contribute power to the grid. Where rates were once established exclusively by (mostly state) regulators, free market forces now provide the basis for much delivered power, though far from all. Consequently, with our fractured system of production, transmission, and consumption of power, stability and reliability are very real issues.

The goal of the power engineer has always been, in its most basic form, to keep the power on. With an ever changing grid, new technologies being invented every day, and the current economic slump, this task is more complicated than it may appear. This thesis explores the intricacies of one type of disturbance to the grid: low frequency, inter-area oscillations.

1.1 Inter-area Oscillation Introduction

Since the 1920's, low frequency electromechanical oscillations have been problematic for power grids across the world. These small oscillations from .1-1 Hz are an anticipated phenomenon which occurs in the grid [2]. They can develop between groups of machines on a network [3]. Fig. 1.1 shows the variation in power of an inter-area oscillation with a 0.4Hz oscillation frequency. Therefore, the power engineer must generate solutions to damp and control these low frequency oscillations before they cause more serious problems in the system.

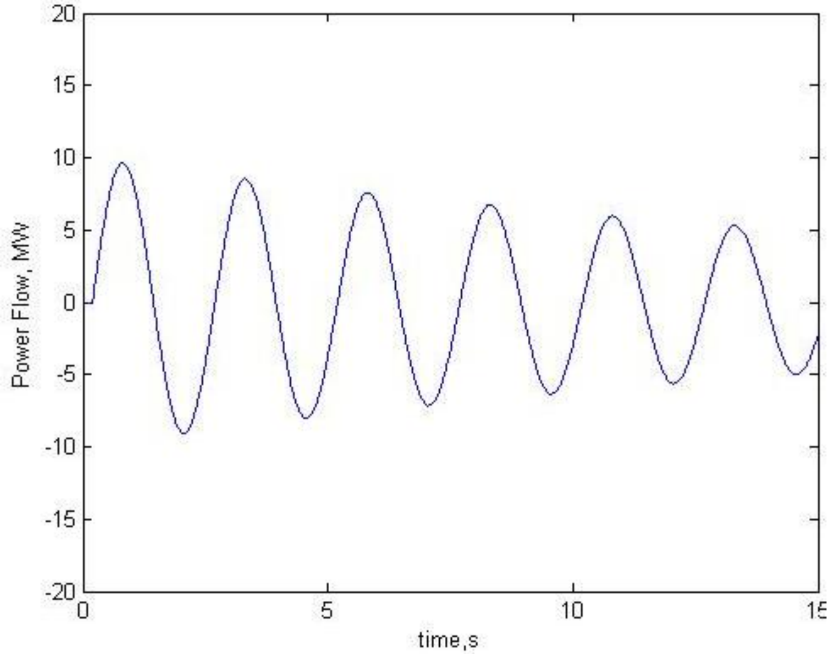

Fig. 1.1 - Inter-area oscillation example

First, the cause of these oscillations needs to be identified. In early grid development, the system was designed to allow for growth. As the system grew rapidly, the transmission network became increasingly stressed and the grid was working closer to transient and small-signal rotor angle stability limits. Insufficient synchronizing torque became a serious cause for system instability. During the mid-century, utilities aimed to increase transient stability with high response exciters. However, in an effort to aid in the first swing transient stability, the low frequency oscillations were exacerbated [3].

These high response exciters create problems for the lower frequency local modes. As the network strength decreases, the exciters can lead to further steady state instability. The first swing would be stable, but then would become unstable. Additionally, because the load was growing faster than anticipated, generator groups began to form. The increase in demand for power weakened the tie lines connecting these generator groups.

The electrical length of the tie lines and the inertia of the machines determine the frequency of the oscillations [3]. In one instance, in a larger interconnection in Canada, the oscillations would generally go undamped until an impedance relay was tripped resulting in the loss of a line [3]. A system operating with lightly damped inter-area modes is stressed [2].

Even in the earlier studies of inter-area oscillations in the 1960s, it was concluded that it was important for dynamic stability problems to be approached as a system wide problem. Synchronous generator excitation and speed control needed to be adjusted based on information from the whole system. Since then, the power industry has advanced greatly, and it has become much easier to design controls which can evaluate the system as a whole.

New developments in remote wide area phasor measurements (WAMS) provide an opportunity for damping these oscillations. Both local and remote measurements can be taken with phasor measurement units (PMUs). These signals are sampled and time synchronized with a precision of one microsecond [4]. Thus, WAMS allow for the synchronized transfer of data across the power network [5]. This means that oscillations can be detected in real-time. Additionally, they can be controlled in real-time with whatever type of control that is chosen or be co-ordinated with a control that is already in place [6]. Therefore, WAMS are an invaluable tool in the control of the modern grid. Additionally, studies have shown that using WAMS to enhance existing controllers is more cost effective than installing new devices [2, 6].

1.2 Solutions

One of the first types of control used for improving steady state stability was the Automatic Voltage Regulator (AVR) [7]. AVRs were used in conjunction with the Power System Stabilizer (PSS) to damp the inter-area modes [7]. The high response exciters, which negatively affected the small signal stability, could be counteracted with this control combination. However, the use of PSSs and AVRs is only a local control. That means that it reacts based on the voltages and angles that it sees locally. Inter-area modes can be only partially damped with this type of control because they are a system wide problem [3].

Flexible alternating current transmission systems (FACTS) have been utilized for increasing the reliability of the grid since the end of the 1980s [8]. They provide a way to control continuously the line impedance, voltage amplitude and angle difference, and other power flow parameters, thereby allowing lines to be loaded to the thermal limit, operate economically, and improve transient stability [2, 9, 10]. Before these devices were invented, many controls implemented in the power system were done mechanically, making them slow and prone to physical failures [10]. The development of FACTS devices is a combination of traditional power system devices (transformers, etc.) and power electronics technology (thrystors, etc.) [9]. They can come in many forms, but the basic implementation involves high power, line-commutated, back to back thyristor valves [10]. Several examples are static VAR compensators (SVCs), thyristor controlled series capacitors (TCSCs), and voltage sourced converter (VSC) systems which include static reactive compensators (STATCOMs) and static series synchronous compensators (SSSCs). However, this thesis will focus mainly on HVDC lines which are a different type of application of power electronic devices.

HVDC lines have been in development for many years now. The first modern HVDC transmission line was built in Sweden in 1954. As of 2000, there have been four 400kV HVDC lines and five back-to-back AC-DC links installed in the U.S. [11]. The basic principle behind HVDC lines is the use of electronic switching valves in a 3-phase bridge configuration to convert AC to DC and back [12]. These lines are appealing from an economic standpoint because they are cheaper to install than an AC line of the same capacity despite requiring converters at both ends of the line [12, 13]. Economic studies have shown that in lines over 600 km, HVDC transmission is more cost effective [11].

Within a stressed system, many of the aforementioned controls cannot maintain stability individually. Combining them provides a more robust way to control the system and prevent blackouts. Common combinations of controls include PSSs with AVRs, with HVDC lines, and with combinations of FACTS devices. These combinations have become possible due to WAMS. When only local measurements were available, the topology of the system could not be observed. Because of this, controls would damp local modes and unknowingly, negatively affect other inter-area modes [14]. By utilizing WAMS, measurements can be applied to local controls to aid in overall system performance [14].

1.3 Linear Matrix Inequalities

The control solutions mentioned above can be implemented with many control techniques. However, for this thesis, linear matrix inequalities (LMIs) were chosen as a way to utilize HVDC lines. The advantage of using LMI's to control the system is that they work for numerous contingencies. This is more appealing than traditional control design, which focuses on developing a control for each individual disturbance, because it is more time and cost effective in addition to being more robust. Furthermore, the LMI control used in MATLAB Robust Control Toolbox can define a multi-objective problem in which the MATLAB program solves for the optimum solution for H_2/H_∞ norms based on a damping region the user defines. The disturbance rejection is attained with the H_∞ control, the control effort is optimized with H_2 control, and the poles are placed with a desired minimum damping ratio [5]. The time delays are represented in the system as uncertain parameters. The control aims to ensure feasibility of the solution, linear objective minimization, and eigenvalue minimization [5].

1.4 Adaptive Control Technique

Originally, MATLAB had an eight case maximum, meaning that there could only be eight contingencies tested. The new version of MATLAB does not have this limitation, but the involved complexity makes it computationally intensive. Additionally, for a large number of contingencies, the optimization may become infeasible [15, 16]. Reference [16] has tried to address this problem by reducing the size of the system. However, by doing so, [16] reduced control over some of the local modes.

This paper presents a different approach for handling such cases. By solving a convex combination of the linear combination of elements consisting of real time sampled inputs and a particular polytopic control, the algorithm will determine which control should be applied to the system at that time. If it is proven to be a convex combination, the program will output constant values. This indicates that the control developed for that polytope will work for that contingency. However, if it is not, the output values will vary widely, indicating that the control will not work for that input. Thus, the proposed algorithm determines which polytopic control is necessary for a particular contingency and classifies the contingency as belonging to a particular polytopic domain. It simplifies the computational complexity of any one problem by breaking it into smaller problems and adaptively choosing the control.

1.5 System Design and Testing

The test system was developed from the New England portion of the IEEE model system. The entire 16 machine model can be found in [17]. This smaller model has eight classically modeled generators and 15 buses with one HVDC line. After splitting the 16 machine system into a smaller one, the load flow was solved using the techniques and programs utilized in [17]. Additionally, the state space representation of the system was determined. Next, the optimal location for the HVDC line was found by computing the lowest frequency modes and analyzing the real part of the participation factors of the generator speeds.

Now that the system formulation is complete, it is necessary to explain the control techniques applied. First, the robust LMI control was applied to two different polytopes created from this system. This control was found to successfully damp the individual polytopes. It was also tested on all of the test cases used in creating each polytope to ensure that all of the contingencies could not be damped by one controller. However, the LMI control could not damp all of the test cases. This is important to note because if it were able to damp all the test cases, there would be no need to break them into separate groups. Additionally, the adaptive testing would return a positive result for each test because all of the test inputs would be damped by the control.

Next, one polytope was selected for the adaptive algorithm and a test case belonging to it was chosen as the input. A recursive algorithm was solved to determine if the input and the controlled system formed a convex combination. This was proven to be true. Then, when a test case from the other polytope was chosen as the input, the output indicates that it is not a convex combination. This means that the selected control is not valid for that polytope, as was expected.

1.6 Outline of Thesis

This thesis is organized in the following manner:

Chapter 1: Introduction

This introduction provides a brief history of the electrical industry and how the problem of inter-area oscillations arose. Additionally, information about the mathematical background, problem formulation, and system testing were discussed.

Chapter 2: Inter-area Oscillations and Solutions

This chapter explores the different solutions to the problem of inter-area oscillations. It looks at some basic pros and cons of the different technologies and how they can be integrated into the system. It further explores HVDC lines and how they operate in the system.

Chapter 3: Linear Matrix Inequalities

This chapter explains the mathematical formalities of LMIs and why they help provide a robust control technique. Their multi-objective solution is discussed.

Chapter 4: Adaptive Control Technique

This section investigates the adaptive control developed to overcome the inadequacies of just using LMIs to solve for a system control. It will further discuss the implications and theory of a convex combination.

Chapter 5: Problem Formulation and Testing

This will provide information on how the system was developed and how the controls were placed. Details about the state space formulation of the system will be further explored. It explains how and why the different contingencies were chosen. It will also show the results of the different controls applied to each system. It shows the outputs of the adaptive control algorithm and how that control will work if it is applied to the input signals.

Chapter 6: Conclusions and Future Work

This chapter briefly reviews the findings of this research and their implications. Additionally, future work plans are discussed.

Chapter 2 – Damping Inter-area Oscillations

This chapter introduces key terms in this thesis. Power system stability is detailed in a high level manner. Additionally, electromechanical oscillations, and specifically inter-area oscillations, are discussed. The linearization of power systems and implication of this process is explained as well. This is followed by a description of the different types of controls that can be utilized to damp inter-area oscillations with HVDC controls explored in more detail.

2.1 – Power system stability

The goal of this thesis is to ensure the stability of the power system. This requires a well defined understanding of power system stability. Most recently, system stability was defined by [18]:

"Power system stability is the ability of an electric power system, for a given initial operating condition, to regain a state of operating equilibrium after being subjected to a physical disturbance, with most system variables bounded so that practically the entire system remains intact."

Additionally, because synchronous generators produce most of the power generated in the system, these generators must be kept in synchronism [18]. Power system stability can be grouped into two categories: small signal stability and transient stability. Small signal, or steady state, stability reflects the system's resilience to small disturbances. It ensures that the difference in the phase angles across transmission lines is not too large and that bus voltages are near nominal values [19]. Transient stability denotes the ability to regain stability after a larger event. These events could include loss of generation or large changes in load. The focus of this thesis is on steady state stability. Small disturbances are the main cause of the inter-area oscillations that we aim to damp. Moreover, this study evaluates internal stability rather than input-output stability [20]. The input channels are perturbed and evaluated based on the system's components. If the response is bounded, the system is said to be internally stable [2, 21].

2.2 – Power system oscillations

Let us now discuss the different types of power system oscillations. The types of oscillations are determined by the part of the power system affected by them. The electromechanical oscillations are studied particularly because they affect small signal stability. The following is a list of several types of electromechanical oscillations [2]:

- Intra-plant mode oscillations
  - Intra-plant mode oscillations occur when machines on the same bus oscillate against one another at a frequency of about 2.0-3.0 Hz.
  - Torsional modes between rotating plants
    - These are much higher frequency modes in the range of 10-46 Hz which are associated with the turbine generator shaft. These can occur when a multi-stage turbine generator is connected to the grid through a series compensated line.
  - Local plant mode oscillations
    - Local modes are caused by one generator swinging against the rest of the system at 0.7-2.0 Hz [22]. This oscillation is local to the generator and the line which connects it to the grid, thus allowing the system to be modeled normally. These oscillations can be compensated for with a PSS which modulates the voltage reference of the AVR [2].
  - Control mode oscillations
    - These modes are a side effect of controls placed in the system. They can include poorly tuned SVCs, HVDC converters, exciters and governors.
- Inter-area mode oscillations
  - Inter-area modes are caused by two groups of generators in a network swinging against each other at a frequency of 1 Hz or less [2]. They will be discussed in greater detail below.

2.2.1 – Inter-area Modes

The inter-area modes, which are of particular interest for this thesis, are described in more detail below. As previously stated, inter-area modes are caused by groups of generators in a network swinging against each other at a frequency of 1 Hz or less. The damping of inter-area modes is determined by several factors. These include the tie-line strength, the loads, the power flow through the lines, and the interactions of generators and their controls [2]. Because of the weakening of the system discussed in Chapter 1, it is easy to see how these types of oscillations have become an issue. Additionally, all of the different types of factors which contribute to inter-area oscillations make them difficult to study and understand. In many instances, it is necessary to have a system model to study an inter-area mode [22].

Two types of inter-area oscillations generally occur in large interconnected systems. Very low frequency modes in the range of 0.1-0.3 Hz arise because of all of the system's generators. The other type occurs when the system splits into groups, and the generators in one group swing against another group. These oscillations occur at a slightly higher frequency of approximately 0.4-1.0 Hz [23].

In order to study these modes, it is best to evaluate a small system. The small four-machine, two-area system developed in [22] provides several ways to analyze these modes.

2.3 – Linearity in Power Systems

Because many of the components in a power system are characteristically explained by differential algebraic non-linear equations, the computational complexity associated with them is high. These include generators, excitation systems, governors, and loads. For a small system, the non-linear control techniques can be applied, but when the system grows, it is not practical to solve such a problem.

However, for the purposes of this thesis, linear control theory can provide useful information about the system. When low frequency oscillations occur due to small disturbances, they are approximately linear [2]. A small disturbance is also one in which the system dynamics can be linearized [10]. The differences in machine angles and speeds are small when disturbances such as small fluctuations of generation and load occur. The differential algebraic non linear equations can be linearized with respect to a system equilibrium point. For more information about the linearized system equations, see [10, 2, 24, 25].

Additionally, by describing a power system as a set of linear equations, modal analysis can be performed to determine information about the system oscillations. This will be described in detail in Chapter 5.

2.4 – Control in Power Systems

It is now necessary to evaluate the requirements of a controller in power systems. A robust control system is one which has little to no sensitivity to the difference between the actual system and the model used for designing the control. Robustness requires the control to provide adequate damping and a security margin during all operating conditions [2].

[2] provides a concise explanation of the necessary control design specifications in power systems that ensure the adequate performance, stability, and robustness.

1. Critical modes must maintain a minimum damping ratio.
2. Based on utility guidelines, all oscillations must settle within a particular time.
3. The robustness measure of performance and stability margins require that the damping must not decrease to unacceptable levels during varying operating conditions and network configurations.
4. There should be no adverse interaction between controllers for different devices (i.e. they should be coordinated through multivariable control design).

Additionally, the control system must include performance objectives which make the system respond in a desirable manner. The rise time, settling time, steady state offset, gain and phase margins are indications of performance. These can be characterized in either the time domain or the frequency domain.

2.4.1 – Power System Control Options

Many different types of power system controllers exist. The following is a brief introduction into several of the more common varieties.

There are several classical controls which are used in power systems. These include Automatic Voltage Regulators (AVRs) and Power System Stabilizers (PSSs).

An AVR is used in local control elements. It can regulate the generator terminal voltage through control of the amount of current supplied to the generator field winding by the exciter. In order to regulate the field current and the exciter output, the voltage measured at the generator terminal is compensated for by the load current. The generator terminal voltage is compared to the desired voltage reference. The difference in the generator terminal voltage and the desired reference voltage is what alters the field current and exciter output. Therefore, the difference is decreased to zero. It is a closed-loop system [10].

A PSS control is one of the traditional forms of controls currently in use in Power Systems. This device is added to an AVR loop to improve damping during power swings. It provides a component of the electrical torque in the synchronous machine rotor which is proportional to the deviation of the actual speed from the synchronous speed. This means that when the rotor oscillates, the torque damps the oscillation [2]. The commonly used stabilizing signals include shaft speed, terminal frequency, and power [10]. Although PSSs are common forms of control, they are mostly used for damping local modes. They can actually have a negative effect on inter-area modes if used inappropriately [26]. An example of an inappropriate use would be when the PSS sees an oscillation and operates, even though that mode is not actually a problem for the system. If it could see the whole system, the PSS would not apply its control and would not damp that mode. The negative effects of the PSS can be mitigated by integrating wide area measurements into the system and only acting when the mode is detrimental to the system as a whole [26, 24].

Flexible AC Transmission Systems (FACTS) devices developed from thyristor based technologies help to improve system stability. They are solid state designs that are being applied to power systems to increase stability. They can provide fast, continuous control over the power flows in a system such that generators and load shedding may not be needed to maintain system stability [2]. Additionally, they provide a way to change the power flows so that they are optimal for the equipment and the economic dispatch is obeyed [2].

SVCs – Static VAR Compensators (SVCs) have been utilized since the 1970s, even though FACTS devices were not developed at that time. The basic principle behind SVCs is to provide reactive power compensation when the system is in need. It includes both capacitive and inductive elements that can be introduced quickly to adjust to rapidly changing loads. The generic SVC is composed of a thyristor controlled reactor and a fixed capacitor.

TCSC – A Thyristor Controlled Series Capacitor (TCSC) is another common FACTS device. It is a capacitive reactance compensator consisting of a series capacitor bank shunted by a thyristor controlled reactor. The goal is to smooth the variations in series capacitive reactance [2]. This is done by changing the firing angles which changes its apparent reactance.

ESD – An Energy Storage Device (ESD) can help to stabilize and improve the reliability of the power system. Examples of these include flywheels, advanced capacitors, and battery energy storage systems. Rather than supplying reactive power, these devices can provide real power to the system rapidly and without detrimentally impacting power flow. There is research currently being done at Virginia Tech about the placement of these devices in power systems [26].

Coordinated Controls – Although each individual device can provide some form of control in a power system, the benefits of combining these controls are being further explored. With multiple controls in place, damping all of the inter-area modes becomes a more realistic goal. Coordinated control is not possible without Wide Area Measurements (WAMS) which are provided by Phasor Measurement Units (PMUs).

There are several papers which provide information on their studies of coordinated control. In [27], the coordinated control of TCSCs and SVCs was developed for increasing damping of inter-area oscillations with successful results. [16] and [28] also explore different types of coordinated controllers.

2.4.2 Information on HVDC lines

The development of HVDC (High Voltage Direct Current) transmission systems was facilitated in the 1930s with the invention of mercury arc rectifiers. In 1941, work on HVDC transmission systems had begun in Germany. However, because of WWII, no system actually was implemented. In 1954 the first HVDC transmission system came to fruition in Gotland, a large island province of Sweden. By the 1960s, HVDC transmission systems had evolved into a mature technology.

These systems can play a vital part in both long distance transmission and in the interconnection of systems. HVDC transmission systems combine high reliability with a long useful life. They must include a power converter to interact with the AC transmission system. Conversion back and forth between AC and DC occurs using controllable electronic switches (valves) in a 3-phase bridge configuration. Generic HVDC converters have capacitors at both ends for reactive power compensation. There is real power input at one end and it exits to a load at the other end.

Additionally, HVDC lines are advantageous because they do not have problems that are associated with AC lines, namely [29]:

- No length limit
- No synchronism requirement
- No increase to short circuit capacity imposed on AC switchgears
- Not affected by impedance, phase angle, frequency, voltage changes
- Improves AC system reliability, thereby increasing carrying capacity by modulating power in response to power swings or frequency fluctuation

Unlike AC lines, the transmission on HVDC lines is not limited by reactive power constraints [13]. They cannot become overloaded because the power flow through them is controlled, meaning that they do not have to be sized to handle a contingency reserve [13].

2.4.2.1 – Economic & Environmental Benefits

Economics plays a major role in the selection and use of HVDC technology [30]. The cost of a DC transmission line varies from 80% to 100% of the cost of an AC line with the same rated line voltage. However, over long distances, DC transmission may be rated at twice the power flow capacity of an AC line of the same voltage.

AC lines no longer become a viable option for transmission over long distances underground or under water on a technical basis. Capacitive charging current associated with AC is the reason for this. [30] states the critical length at which DC becomes a viable choice is 50 km. The DC line must be at least 50km because the converters at each end are expensive. If the line is too short, it is not more economically advantageous than AC lines. The economic benefits of DC lines are part of the appeal for studying them as a plausible technique for power system control.

Additionally, there are several environmental benefits to using DC lines. These can be separated into two categories. One set of effects is those associated directly with the flow of current in the power lines. A second set of effects consists of those caused by the mere presence of power lines in the environment [30].

Effects arising from the presence of power in transmission lines may be separated into field and ion effects and corona effects. Power lines produce both electric fields and charged airborne particles. There has been concern that either the fields or the charged particles emitted at low levels may cause detrimental health effects. However, epidemiology studies do not generally support these concerns.

The second set of environmental issues arises in connection with the mere siting of power lines in the outdoor environment. Because power lines are large physical structures which occupy a lot of space, people in the communities which host them believe they negatively impact the atmosphere. These range from aesthetic concerns, negative effects on property values in their vicinity, obstruction of view, and cultural issues to transportation hazard, wetlands impacts, deforestation, and harm to water resources. The comparative footprint of AC and DC power lines merits discussion. For the same amounts of power transmission, DC power lines occupy less land than AC lines. Taking less land means less cost for transmission line construction. It may mean less public opposition, as well.

The information given is just to provide a small introduction to HVDC lines and why they are a viable option for power system control. It is important to evaluate the different aspects of a technology before studying it to ensure that it is not only for the intellectual pursuit, but also for practical purposes. The more general purpose of this chapter was to explain some of the basic tenets of the power system stabilization problem and provide information needed for understanding this thesis as well as to provide resources for further details on related topics.

Chapter 3 – Linear Matrix Inequalities

Linear matrix inequalities (LMIs) provide an incredibly powerful way to solve convex or quasi convex optimization problems [31]. There is a long history of using LMI controllers in many different fields ranging from robotics, to electronics, to aerospace application. Their ability to provide robust control is constantly being proven. Many control problems require both performance and robustness objectives which can be solved using the LMI control because it allows for multi-objective optimization.

The first LMI appeared in the analytical solution of the Lyapunov equation in 1890. After that it was not until the 1940s that small LMI problems were beginning to be solved by hand by applying Lyapunov's methods. From the 1960s to the 1980s, more algorithms to solve LMIs were created. These numerical algorithms enable the use of LMIs in solving control problems.

LMIs intrinsically reflect constraints, not optimality, which is one reason why they can combine multiple constraints on the closed loop system [27, 31, 32, 33]. Additionally, they allow for problems to be solved numerically via semidefinite programming (SDP) with interior-point methods in the Robust Control Toolbox in MATLAB. Prior to the development of interior point methods, other algorithms were employed such as the method of centers to solve for the mixed controls. This provides an alternative to the classical analytical solutions which may be impossible to find when multiple constraints or objectives are defined [34].

The basic principle of this problem lies in evaluating the Lyapunov stability criterion. Not only can his methods indicate system stability, but they also can be used to find bounds on system performance. This is assuming the system performance does not need an analytical solution [31]. The multiple objectives can be met with H_∞ for disturbance rejection, H_2 for control effort optimization, and pole placement for the desired damping. All of these can be achieved by using LMIs to create a multi-objective, suboptimal control problem [2].

3.1 Basic Form of a LMI

An LMI is any constraint in the following form [31]:

$$F(x) \coloneqq F_0 + \sum_{i=1}^{m} x_i F_i < 0 \tag{3.1}$$

where

- $\mathrm{x} = \mathrm{x}_1, \mathrm{x}_2, \ldots \mathrm{x}_\mathrm{m} \in \mathrm{R}^\mathrm{m}$ is an unknown vector of scalar optimization variables
- $\mathrm{F}_1, \mathrm{F}_2, \ldots \mathrm{F}_\mathrm{n}$ are known symmetric matrices, *i.e.* $F_i = F_i^T \in \boldsymbol{R}^{nxn}$, $i = 0, \ldots, m$ are given
- < 0 inequality indicates that $F(x)$is negative definite. This means that the largest value of $F(x)$ is negative. This can also be shown by the inequality:
    - $u^T F(x) u < 0$ for all nonzero $u \in \boldsymbol{R}^n$

The LMI defined in (3.1) is a convex constraint on x because $\mathrm{F(y)} < 0$ and $\mathrm{F(z)} < 0$ imply $\mathrm{F}\left(\frac{\mathrm{y+z}}{2}\right) < 0$. Thus,

- The LMI is a convex constraint on x meaning that the set $\{x | F(x) < 0\}$ is convex.
- The solution set is called the feasible set and is a convex subset of $\boldsymbol{R}^n$.
- The solution, x, to $F(x)$ is a convex optimization problem.
- An LMI is a set of *n* polynomial inequalities in *x*.

Because (3.1) is convex and has no general solution, it can still be solved numerically. If an answer is feasible, it can be found and it is guaranteed to be optimal. Additionally, it is very significant that multiple LMI constraints can be regarded as a single LMI.

This can be seen in (3.2).

$$\begin{cases} F_1(x) < 0 \\ \vdots \\ F_K(x) < 0 \end{cases} \quad is\ equivalent\ to\ F(x) \coloneqq diag\big(F_1(x), \dots., F_K(x)\big) < 0 \tag{3.2}$$

where

- $diag\big(F_1(x), \dots., F_K(x)\big)$ is the block diagonal matrix with $F_1(x), \dots., F_K(x)$ on the diagonal.
- $\begin{pmatrix} F_1(x) & 0 & 0 \\ 0 & \ddots & 0 \\ 0 & 0 & F_n(x) \end{pmatrix} < 0$

Additionally, note that the convex constraint listed above is very general and can be applied to many types of control problems.

3.1.1 Matrices as variables

When LMIs arise, they tend not to be in the canonical form of (3.1), but in the form:

$$L(X_1, \dots, X_n) < R(X_1, \dots, X_n) \tag{3.3}$$

where

- $L(\cdot) and\ R(\cdot)$ are affine functions of the structured matrix variables $(X_1, \dots, X_n)$.

An example of using matrices as variables is the famous Lyapunov inequality in (3.4).

$$A^T P + PA < 0 \tag{3.4}$$

  - $A \in \boldsymbol{R}^{nxn}$ is given
  - $P_i = P_i{}^T > 0$ is the variable matrix which has $p_1, \dots, p_m$ as independent scalar entries

This can be placed in the form of (3.1) by letting $P_1, \ldots, P_m$ be a basis for nxn matrices where $m = \frac{n(n+1)}{2}$. Set $F_0 = 0$ and $F_i = A^T P_i + P_i A$.

Another important example of this is the *quadratic* matrix inequality given by

$$A^T P + PA + PBR^{-1}B^T P + Q < 0 \tag{3.5}$$

where

- $A, B, Q = Q^T, R = R^T > 0$ are all given matrices and $P = P^T$ is the variable.

It can be expressed as a *linear* matrix inequality as:

$$\begin{bmatrix} -A^T P - PA - Q & PB \\ B^T P & R \end{bmatrix} > 0 \tag{3.6}$$

Equation (3.6) also shows that (3.5) is convex in P [31].

One of the greatest advantages of using an LMI control is the ability to solve multi-objective problems [7]. This will be discussed in the following sections.

3.2 – Definitions and Information to formulate control problems as LMIs

In order to explain some of the following concepts fully, several definitions and lemmas are presented.

3.2.1 – Hurwitz Matrix

A Hurwitz matrix is a time invariant matrix which does not have any eigenvalues s with $Re(s) \geq 0$.

3.2.2 – Well-posed Problem

For the typical optimization problem, the guaranteed existence of an optimal controller given by a feedback gain requires that [35]:

- The pair $(A, B_2)$is stabilizable
- The pair (C_2, A) is detectable
- The system formulation is non-singular.

3.2.3 – Schur Compliment

The Schur Compliment converts nonlinear (convex) inequalities into LMI form. The Schur Lemma follows the basic form for the block matrix as presented in [36]:

$$\begin{pmatrix} Q & S \\ S^T & R \end{pmatrix} > 0$$

If and only if

$$Q > 0 \quad and \quad R - S^T R^{-1} S > 0$$

If and only if

$$R > 0 \quad and \quad Q - S R^{-1} S^T > 0$$

Proof:

$$\begin{pmatrix} I & 0 \\ -S^T Q^{-1} & I \end{pmatrix} \begin{pmatrix} Q & S \\ S^T & R \end{pmatrix} \begin{pmatrix} I & -Q^{-1}S \\ 0 & I \end{pmatrix} = \begin{pmatrix} Q & 0 \\ 0 & R - S^T Q^{-1} S \end{pmatrix}$$

Thus, the set of nonlinear inequalities can be represented as a LMI.

3.2.4 – Bounded Real Lemma

This derivation of the BRL presented below follows the derivation given in [31].

$$\begin{pmatrix} A^TP + PA + C^TC & PB + C^TD \\ B^TP + D^TC & D^TD - I \end{pmatrix} \leq 0 \quad when\ P = P^T > 0$$

In this case: $A \in \boldsymbol{R^{nxn}}$, $B \in \boldsymbol{R^{nxp}}$, $C \in \boldsymbol{R^{pxn}}$, $D \in \boldsymbol{R^{pxp}}$are given, and $P \in \boldsymbol{R^{nxn}}$ is the variable. Assume that A is stable and (A,B,C) are minimal. This means that the LMI is feasible if and only if the LTI system is nonexpansive for all solutions of that LTI where $x(0) = 0$. This is represented as the condition:

$$\int_0^\infty y(t)^T y(t)dt \ \leq \int_0^\infty u(t)^T u(t)dt$$

To be nonexpansive is the equivalent to saying that the transfer matrix satisfies the requirements of the bounded real condition.

$$T(s)^* T(s) \leq I \quad for\ all \quad Re(s) > \ 0$$

Where * denotes the complex conjugate. This can also be shown in the form of an ARE:

$$A^TP + PA + C^TC \ + (PB - C^TD)(I - D^TD)^{-1}(PB - C^TD)^T = 0$$

where $D^TD < I$.

The LMI is feasible if and only if the Algebraic Riccati Equation (ARE) has a solution for $P = P^T > 0$. To solve the ARE, the Hamiltonian matrix can be found. This M must not have any imaginary eigenvalues for the system to be nonexpansive (*i.e.* for the LMI to be feasible).

$$M = \begin{bmatrix} A - B(I - D^TD)^{-1}D^TC & B(I - D^TD)^{-1}B^T \\ -C^T(I - D^TD)^{-1}C & -A^T + C^T(I - D^TD)^{-1}B^T \end{bmatrix}$$

Thus, the matrix P can be obtained by picking a $V \in \boldsymbol{R}^{2n\times n}$ such that the its range is a basis for the stable eigenspace M. This means pick $V = [v_1 \ldots v_n]$ where $v_1 \ldots v_n$ are a set of independent eigenvectors of M associated with its n eivenvalues with negative real parts. Then partition V with two square matrices, V_1 and V_2.

$$V = \begin{pmatrix} V_1 \\ V_2 \end{pmatrix}$$

Then, set the matrix $P = V_2 V_1^{-1}$. Therefore, P is the minimal solution of the ARE.

This information will be helpful in evaluating the H_∞ norm.

3.2.5 – Kalman – Yacubovich-Popov Lemma

This lemma is a combination of the work of Popov in 1962 where he developed a criterion of absolute stability to provide frequency conditions for the stability of nonlinear systems. Later, Yakubovich and Kalman added to Popov's work by identifying the connection between the Popov criterion and the existence of a positive-definite matrix which satisfies certain matrix inequalities [31]. This can also be called the Positive Real Lemma.

Given,

- $A \in \boldsymbol{R}^{n\times n}$
- $B \in \boldsymbol{R}^{n\times p}$
- $C \in \boldsymbol{R}^{p\times n}$
- $D \in \boldsymbol{R}^{p\times p}$
- $M = M^T \in \boldsymbol{R}^{(n+p)(n+p)}$
- $det(j\omega - A) \neq 0 for\ \omega \in \boldsymbol{R}$
- $(A, B) are\ controllable$

The following two statements are equivalent:

1. The frequency domain inequality

$$\begin{pmatrix} (j\omega - A)^{-1}B \\ I \end{pmatrix}^* M \begin{pmatrix} (j\omega - A)^{-1}B \\ I \end{pmatrix} < 0$$

$$\forall\ \omega\ \in\ \boldsymbol{R}$$

2. There exists a matrix $P \in \boldsymbol{R}^{n\times n}$ such that $P = P^T > 0$ and the LMI

$$\begin{pmatrix} A^TP + PA & PB - C^T \\ B^TP - C & -D^T - D \end{pmatrix} \leq 0$$

Except in this case, the equivalent quadratic matrix inequality is:

$$A^TP + PA + (PB - C^T)(D + D^T)^{-1}(PB - C^T)^T \leq 0$$

This is the equivalent of saying the LMI is feasible if and only if the linear system is passive. This is equivalent to saying that the transfer function, $T(s)$, is positive real. Thus,

$$T(s) = C(Is - A)^{-1}B + D \; for \; s \in C$$

and

$$T(s) + T^*(s) \geq 0 \quad for \; all \quad Re(s) > 0$$

By assuming that,

$$D + D^T > 0$$

It is evident that $P = P^T > 0$ is the solution found by solving the ARE:

$$A^TP + PA + (PB - C^T)(D + D^T)^{-1}(PB - C^T)^T = 0$$

The first step in solving for P is forming the Hamiltonian matrix as shown in the Bounded Real Lemma, except in this instance:

$$M = \begin{bmatrix} A - B(D + D^T)^{-1}C & B(D + D^T)^{-1}B^T \\ -C^T(D + D^T)^{-1}C & -A^T + C^T(D + D^T)^{-1}B^T \end{bmatrix}$$

The rest of the process for solving is the same as in the Bounded Real Lemma. For more information on the frequency domain information, see [31].

3.3 – Individual Control Problems

The goal of this control design is to explore multi-objective state feedback. However, it is first necessary to explain the basics of the individual types of control. The types of control used for this design are H_∞ control, H_2 control, and pole placement.

3.3.1 – H_∞ Control

Though some of the earliest work on H_∞ control theory was done in 1971 by Jan Willems, much of the research was conducted in the 1990's. At that time, the H_∞ optimization techniques were a study of the combination of the solvability of the Riccati equations and the bounded real lemma [31]. From there, researchers including, but not limited to, Carsten Scherer, Pascal Gahinet, and John Doyle continued to push the boundaries of this problem by posing the problem as a state space problem with convex constraints. Eventually, these controllers were able to be formed in terms of LMIs. In [33], it is stated that the H_∞ synthesis can be formulated as a convex optimization problem by using LMIs. In this case, the LMI corresponds to the inequality counterpart of the H_∞ Riccati equations.

In a system, the H_∞ norm is the largest magnitude of the transfer function over the whole frequency range. Essentially, this value indicates the maximum gain in the principal direction. Another way to phrase this is that the H_∞ norm is the magnitude of some loop transfer function in the worst direction over the entire frequency range [2]. In order to minimize the effects of a disturbance, it is necessary to minimize the H_∞ norm. The H_∞ norm is the maximum of any component in the space. It is commonly called the maximum norm [2]. This is why it is a common problem to try to minimize this maximum value. The minimization of the $\boldsymbol{H_\infty}$ norm is a commonly used tool for designing feedback controllers because it allows for loop-shaping and robustness when plant modeling errors are present [35].

3.3.1.1 – Mathematical Exploration of H_∞ Control

In order to understand the H_∞ norm, it is necessary to start with the generic linear input-output system given by (3.7).

$$\begin{pmatrix} \dot{x} \\ y \end{pmatrix} = \begin{pmatrix} A & B \\ C & D \end{pmatrix} \begin{pmatrix} x \\ u \end{pmatrix} \tag{3.7}$$

where

- $x(t)$ is the state vector.
- $u(t)$ is the input vector.
- $y(t)$ is the output vector.
- $x(0) = 0$ is the initial condition.

From (3.7), the transfer function in (3.8) is formed.

$$T(s) = C(sI - A)^{-1}B + D \tag{3.8}$$

From this, the basic principle behind the H_∞ norm can be determined. It measures the system input-output gain for finite energy (or finite root mean square, RMS) input signals [36]. The $\boldsymbol{H}_\infty$ norm is the peak gain across frequency in the single value norm. It could also be explained as the magnitude of a loop transfer function in the worst direction across the entire frequency range [2]. The $\boldsymbol{H}_\infty$ norm $\|T\|_\infty$ of the transfer matrix T, is defined as:

$$\|T(s)\|_\infty = \sup_{\omega > 0} \bar{\sigma}(T(j\omega)) \tag{3.9}$$

where

- $\bar{\sigma}(T(j\omega))$ is the largest singular value of T

Additionally, if the LTI system in (3.7) is asymptotically stable and the maximum singular value of the transfer function (3.8) is bounded by $\gamma > 0$, there are desirable time domain properties as well. One way to think of an asymptotically stable system is a system which is stable if every initial state x_0 causes a bounded system response that approaches 0 as $t \to \infty$. This means that the pair of real matrices (A, B) is stabilizable such that there exists a K such that $A + BK$ is a Hurwitz matrix. Additionally, the pair of real matrices (C, A) is detectable when (A', C') is continuous time stabilizable [35]. The benefit of these statements is that because A of the transfer function defined in (3.8) is Hurwitz, the L_2 gain of the state space model is the same as the $\boldsymbol{H}_\infty$ norm. Another way of explaining this is that the L_2 gain of the transfer matrix model is equal to the $\boldsymbol{H}_\infty$ norm of the transfer matrix. For a proof of this, see [35]. This equation is represented mathematically below in (3.10). It closely follows the derivation in [36].

$$\|T(s)\|_\infty = \sup_{u(t)\neq 0} \frac{\|y(t)\|_2}{\|u(t)\|_2} < \gamma \; \forall \, u \in L_2 \tag{3.10}$$

This right side of this expression defines the input-output relation and is equivalent to the quadratic condition given in (3.11a)-(3.11b).

$$\|y(t)\|_2^2 - \gamma^2 \|u(t)\|_2^2 = \int_0^\infty y(t)^T y(t) - \gamma^2\, u(t)^T u(t) dt < 0 \tag{3.11a}$$

Alternatively,

$$\int_0^\infty \begin{pmatrix} y \\ u \end{pmatrix}^T \begin{pmatrix} (\gamma I)^{-1} & 0 \\ 0 & -\gamma I \end{pmatrix} \begin{pmatrix} y \\ u \end{pmatrix} dt \tag{3.11b}$$

If the substitution for $y(t) = Cx(t) + Du(t)$ is made, (3.11a, 11b) can be reformed as:

$$\int_0^\infty \begin{pmatrix} x \\ u \end{pmatrix}^T \underbrace{\begin{pmatrix} C & D \\ 0 & I \end{pmatrix}^T \begin{pmatrix} (\gamma I)^{-1} & 0 \\ 0 & -\gamma I \end{pmatrix} \begin{pmatrix} C & D \\ 0 & I \end{pmatrix}}_{M} \begin{pmatrix} x \\ u \end{pmatrix}^T \tag{3.12}$$

Additionally, supposing that (A, B) is controllable and M is symmetric. The KYP Lemma can be used to find (3.13):

$$\begin{pmatrix} A^T P + PA & PB \\ B^T P & 0 \end{pmatrix} + \begin{pmatrix} \gamma^{-1} C^T C & \gamma^{-1} C^T D \\ \gamma^{-1} D^T C & -\gamma + \gamma^{-1} D^T D \end{pmatrix} < 0$$

$$\begin{pmatrix} A^T P + PA & PB \\ B^T P & 0 \end{pmatrix} + M < 0 \tag{3.13}$$

$$P = P^T > 0$$

Now, using the Schur Compliment, (3.13) can be transformed into (3.14):

$$\begin{pmatrix} A^T P + PA & PB & C^T \\ B^T P & -\gamma I & D^T \\ C & D & -\gamma I \end{pmatrix} < 0 \tag{3.14}$$

This means that the LTI system given by (3.7) is asymptotically stable and $\|T\|_\infty < \gamma$ if and only if $P = P^T$ is the solution to the LMIs in (3.14).

Additionally, we can evaluate the frequency domain inequality where $det(j\omega - A) \neq 0 \forall\ \omega \in \boldsymbol{R}$ is

$$[C(j\omega I - A)^{-1} B + D]^* [C(j\omega I - A)^{-1} B + D] - \gamma^2 I < 0$$

Which is equivalent to:

$$\|C(sI - A)^{-1} B + D\|_\infty < \gamma$$

To make the final equations relate explicitly to the $\boldsymbol{H}_\infty$ norm as explained in this section, the P for which we are solving, will be replaced with P_∞. The LTI system will be modified slightly so that the state equations are:

$$\begin{aligned} \dot{x} &= Ax + B_1\omega + B_2 u \\ z_\infty &= C_1 x + D_{11}\omega + D_{12} u \\ y &= C_y x + D_{y1}\omega + D_{y2} u \end{aligned} \tag{3.15}$$

The state-feedback model can be found with Fig. 3.1. In this case, $T(s)$is the LTI system.

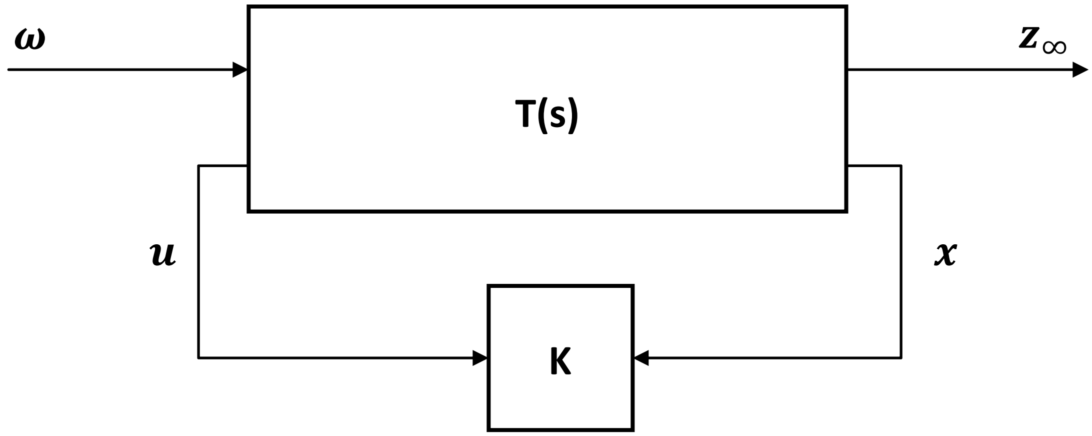

Fig. 3.1 – State Feedback model for z_∞

Therefore, the closed loop matrices are, for $u = Kx$:

- $A_{cl} = A + B_2 K$
- $B_{cl} = B_1$
- $C_{cl\infty} = C_1 + D_{12} K$
- $D_{cl\infty} = D_{11}$

The resulting LMI formed is (3.16):

$$\begin{pmatrix} A_{cl}{}^T P_\infty + P_\infty A_{cl} & P_\infty B_{cl} & C_{cl\infty} \\ B_{cl}^T P_\infty & -\gamma I & D_{cl\infty}^T \\ C_{cl\infty} & D_{cl\infty} & -\gamma I \end{pmatrix} < 0 \qquad with \qquad P_\infty = P_\infty^T > 0 \qquad (3.16)$$

Now that the mathematical derivation is complete, H_∞ synthesis is desirable because by maintaining H_∞ bounds, robust stability and noise attenuation can be achieved [37]. It provides disturbance rejection by minimizing the closed loop RMS gain [14].

3.3.2 – H_2 Control

The history of H_2 control lies in the exploration of the Linear Quadratic Gaussian (LQG) control problem. This in itself is an expansion of the Linear Quadratic Regulator (LQR) control problem. N. Wiener pioneered the work of linear quadratic control during WWII when using a mean-square technique for firing control of weapons. The term "linear" originates from the use of linear systems, and "quadratic" stems from the use of performance measures which use the square of the error signal. Prior to the late fifties, the linear quadratic problem was commonly referred to as the mean square control problem [38].

This type of optimization was appealing because it did not use the trial and error approaches formally utilized by the Nyquist stability criterion. Additionally, it accounted for sensor noise and control input saturation. By the late 1950s, Kalman worked on generalizing the performance measures of this type of control. This led to the development of the quadratic performance measure and the LQR problem. In the 1960s, Kalman and Bucy developed a new state variable filter [39]. This was the start of the design for an LQG problem which accounts for stochastic disturbance signals [38].

The principle behind solving linear quadratic problems is finding a controller K that minimizes the cost function, *J*. This is a part of the Lyapunov stability criterion. It is a useful construct for stability analysis in LTI systems. The Lyapunov inequality is:

$$A^T P + PA < 0 \quad for \quad P = P^T > 0$$

This LMI can be solved for any chosen $Q = Q^T > 0$. If the system $\dot{x} = Ax$ is stable, the linear equation $A^T P + PA + Q = 0$ has the solution for P such that it is positive and finite. This problem can be written as a SDP problem. It can also be written as an LMI optimisation problem. The following flows from an example in [36]. Given

$$\dot{x(t)} = Ax(t) \quad where \quad x(0) = x_0$$

There is a resulting cost function:

$$J = \int_{0}^{\infty} x^T(t)Qx(t)dt < \infty \;\; such\ that \quad Q = Q^T > 0$$

This means that the system is asymptotically stable because $J < \infty$. The proof is as follows. First, set up a quadratic Lyapunov function:

$$V\big(x(t)\big) = x^T(t)Px(t)$$

$$P = P^T > 0$$

The equation will become:

$$\frac{dVx(t)}{dt} = \frac{d}{dt}\big(x^T(t)Px(t)\big) \leq -x^T(t)Qx(t)dt$$

This equation is negative definite for all trajectories, as well as all values of t. When the LMI feasibility problem is solved, a P that bounds J can be found. This P can be optimized by determining the smallest bound. The resulting equation is the integral from $t = 0\ to\ t = T$.

$$x^T(T)Px(T) - x(0)^T Px(0) \leq -\int_0^T x^T(t)Qx(t)dt$$

It is known that $x^T(T)Px(T) \geq 0$ and that this is correct for $t \to \infty$. It can be represented as

$$J = \int_0^\infty x^T(t)Qx(t)dt \leq x^T(0)Px(0)$$

Thus, the cost function is bounded. This is described in the equation below.

$$J \leq x_0^T P x_0$$

By differentiating, it is seen that

$$\frac{d}{dt}\big(x^T(t)Px(t)\big) = x^T(t)(A^T P + PA)x(t) \leq -x^T(t)Qx(t)$$

$$A^T P + PA + Q \leq 0$$

Therefore, by finding a $P = P^T$ which provides a bound on J is solved with an LMI feasibility problem. Additionally, it can be optimized over P by searching for the lowest bound. This is an semi-definite programming (SDP) problem. Using interior point methods, it can be evaluated numerically. The problem can be seen as the solution to the following:

$$\min x_0^T P x_0$$

$$subject\ to\ P > 0\ A^T P + PA + Q \leq 0$$

This is just the basics for information on solving a minimization problem with linear matrix inequalities for reference purposes. It should be kept in mind that the point of solving these problems is to minimize the cost function. For more information see [31,36].

The following information is focused on the H_2 problem more specifically. When the LQG problem is evaluated in the frequency domain, it is commonly called the H_2 control problem. This is because, in the frequency domain, the performance measure corresponds to the time domain LQG measure [38]. The H_2 norm for a stable transfer function is defined as:

$$\|T(s)\|_2 = \sqrt{\frac{1}{2\pi} \int_{-\infty}^{+\infty} \{tr(T(j\omega)^* T(j\omega)\} \, d\omega} \tag{3.17}$$

Where $\|T(s)\|_2 = \infty$ if there are poles on the imaginary axis. When T does not have any poles s with $Re(s) \geq 0$, the L_2 is the same as the H_2 norm [35].

In the H_2 optimization problem, for a given plant, P, the feedback controller, K, provides a well posed, stable connection which minimizes the H_2 norm of the closed loop transfer function T. One way of thinking about the H_2 optimization problem is that it minimizes the sensitivity of the output z_2 to the white noise input of ω [35]. The overall energy of a system relating input disturbance to output response is measured by the H_2 norm [2]. The H_2 performance ensures the optimal output performance [36].

The H_2 norm of the transfer function $T(s)$ is found by taking the following steps. The transfer function is defined by (3.18).

$$T(s) = C(sI - A)^{-1}B + D \tag{3.18}$$

The H_2 norm is determined by taking the integral of $T(s)$ over a range of frequencies. This expression is given in (3.19).

$$\|T(s)\|_2 = \sqrt{\frac{1}{2\pi}\int_{-\infty}^{+\infty}\{tr(T(j\omega)^*T(j\omega)\}\,d\omega} \tag{3.19}$$

Parseval's Theorem states that $\|T(s)\|_2$ is H_2 norm of the impulse response given in (3.20).

$$\|T(s)\|_2 = \|t(t)\|_2 = \sqrt{\int_0^\infty trace\left(t^T(t)t(t)\right)dt} \tag{3.20}$$

The impulse response of the matrix is given by:

$$t(t) = \begin{cases} 0, & t < 0 \\ Ce^{At}B + D\delta(t), & t \geq 0 \end{cases} \tag{3.21}$$

For a strictly proper transfer function T, which implies that A is Hurwitz and D = 0, equations (3.22a)-(3.22b) are given.

$$\|T(s)\|_2^2 = trace\left\{B^T\int_0^\infty e^{A^Tt}C^TCe^{At}dt\;B\right\} = trace(B^TQ_2B) \tag{3.22a}$$

$$\|T(s)\|_2^2 = trace\left\{C^T\int_0^\infty e^{At}BB^Te^{A^Tt}dt\;C^T\right\} = trace(CP_2C^T) \tag{3.22b}$$

P_2 is the solution to the controllability grammian for the Lyapunov equation:

$$A_{cl}P_2 + P_2A_{cl}^T + B_{cl}B_{cl}^T = 0 \tag{3.23}$$

Q_2 is the solution to the observability grammian for the Lyapunov equation:

$$A_{cl}^TQ_2 + Q_2A_{cl} + C_{cl}^TC_{cl} = 0 \tag{3.24}$$

Therefore, upon finding the solution for $P_2 > 0$ and $Q_2 > 0$, one can say that:

$$A \text{ } is \text{ } Hurwitz \text{ } and \text{ } \|T(s)\|_2^2 < \nu$$

$$trace(CP_2C^T) < \nu \quad and \quad A_{cl}P_2 + P_2A_{cl}^T + B_{cl}B_{cl}^T < 0$$

$$trace(B^TQ_2B) < \nu \quad and \quad A_{cl}^TQ_2 + Q_2A_{cl} + C_{cl}^TC_{cl} < 0$$

Where

$$A_{cl} = A + B_2K$$

$$B_1 = B_{cl}$$

$$C_{cl2} = C_2 + D_{22}K$$

$$D_{cl2} = D_{21} = 0$$

In order to formulate this in LMI terms, the Schur Complement must be invoked. The LMI formulation is in (3.25).

$$\begin{pmatrix} A_{cl}P_2 + P_2A_{cl}^T & B_{cl} \\ B_{cl}^T & -I \end{pmatrix} < 0$$

$$\begin{pmatrix} Q_2 & C_{cl}P_2 \\ P_2C_{cl}^T & P_2 \end{pmatrix} > 0 \tag{3.25}$$

$$trace(B^TQ_2B) < \nu$$

$$P_2 = P_2^T > 0$$

$$Q_2 = Q_2^T > 0$$

These equations provide the global minimum of the LMI problem for $\|T(s)\|_2^2$. This section provided a mathematical explanation of the H_2norm and how it is used with LMIs. For further information on the effects of Gaussian noise on the H_2 problem, see [31, 35, 38].

3.3.3 – Pole placement and eigenvalue minimization

First, it is necessary to address the reason why poles need to be placed in a particular region, and then where they need to be placed. The location of poles in a control problem is an indication of the stability of the system. In order for a system to be stable, all of the poles of that system must be in the left-hand plane of the real and imaginary axis. In order to ensure maximum damping, it is necessary to keep these poles at least a certain distance away from the axis. The step response of a second order system with poles allows us to see how this region can be formed. The equation (3.26) represents a complex pole in real and imaginary parts.

$$\lambda = -\zeta\omega_n \pm j\omega_d = -\sigma \pm j\omega_d \tag{3.26}$$

Where

- ζ is the damping ratio
- $\omega_n = |\lambda|$ is the undamped natural frequency and is an indication of rise time
- ω_d is the damped natural frequency
- σ is the real part of the pole

These particular regions must be defined for the application in question:

- $Re(s) \leq -\sigma$
  - Which ensures a minimum decay rate; it indicates the settling time
- $\zeta = cos\theta$
  - Which creates a minimum damping ratio of ζ, which is an indication of the overshoot of the system response
- $\omega_d = r\ sin\theta$
  - Which creates a maximum undamped natural frequency of ω_d

With these conditions set, the bounds for maximum overshoot, frequency of oscillating modes, delay time, rise time, and settling time are determined [33, 40]. These can be explained as the set $S(\sigma, r, \theta)$ of the complex numbers $z = x + jy, where\ x = Re(z)\ and\ y = Im(\bar{z})$. The variable $\overline{z}$ is the complex conjugate of z. This can be formulated such that:

$$x < -\sigma < 0, \qquad |x + jy| < r, \qquad tan\theta x < -|y| \tag{3.27}$$

These more complicated regions are the intersection of individual LMI regions [41]. A picture of this region can be seen in Fig. 3.2.

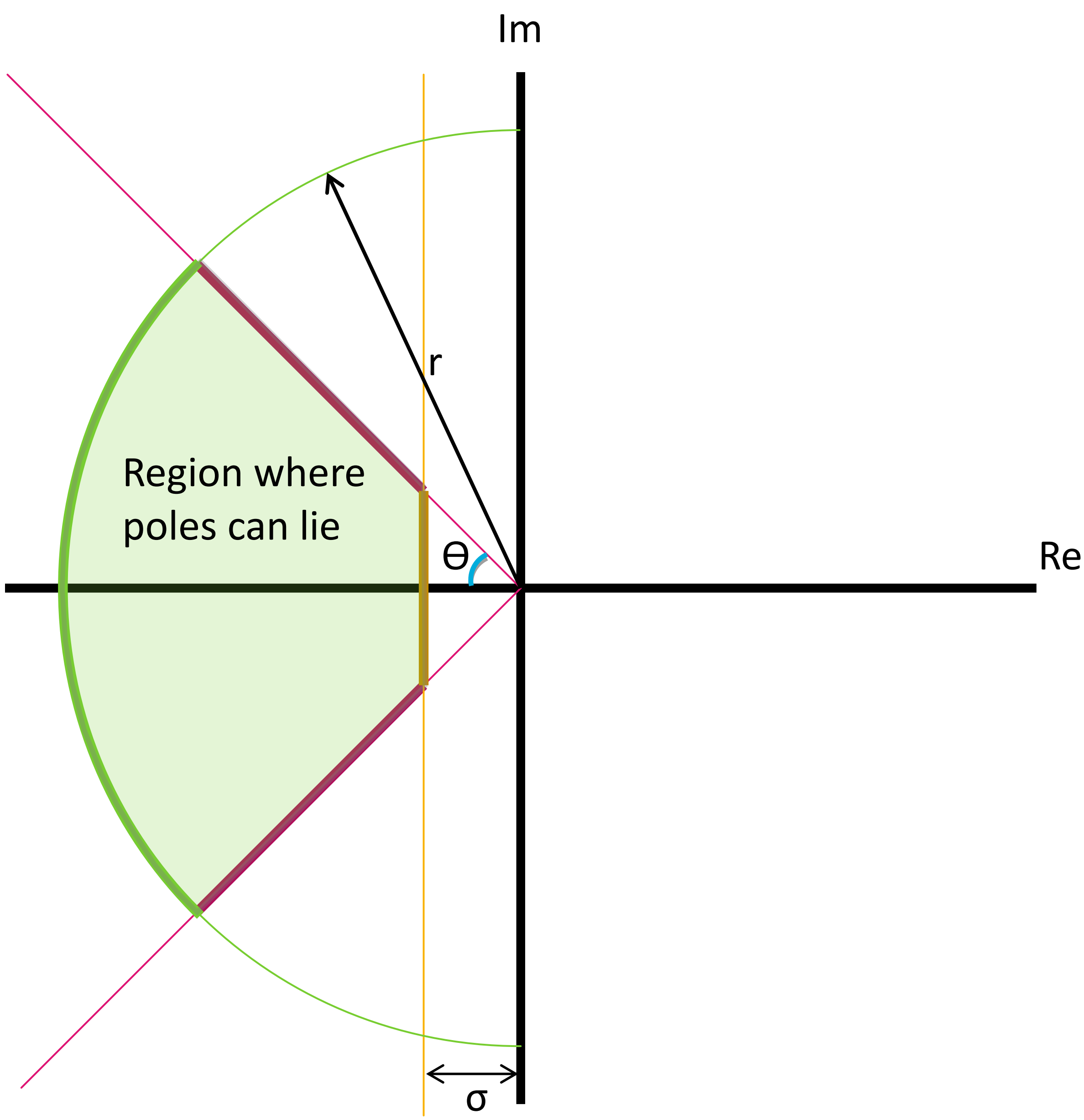

Fig. 3.2 - The region $S(\sigma, r, \theta)$

To further explain this in LMI terms, it is necessary to have the LMI regions be convex subsets D of the complex plane. This is defined by the following equation:

$$D = \{z \in \boldsymbol{C}: \; f_D(z) < 0\} \tag{3.28}$$

The characteristic function of this region, D, is given by the matrix valued function:

$$f_D(z) \coloneqq \alpha + \beta z + \beta^T \bar{z} \tag{3.29}$$

Where $\alpha = \alpha^T = [\alpha_{ij}] \in \boldsymbol{R}^{mxm}$ and $\beta = [\beta_{ij}] \in \boldsymbol{R}^{mxm}$ are fixed matrices. The inequality < 0 makes it negative definite. This function has value in the space of mxm Hermitian matrices [31]. It is also important to note that LMI regions are symmetric with respect to the real axis because for any $z \in D$, $f_D(z) = \overline{f_D(z)} < 0$ [33].

When the region, D, encompasses the entire left hand plane, it is an indication of asymptotic stability. It is important to note that because the original region is convex, the intersection of these convex regions creates a convex region [31]. Therefore, arbitrary LMI regions in the open left half plane can be found from generalizing the Lyapunov theorem for the open left-half plane where $\{z: z + \bar{z} < 0\}$ [42]. The A matrix only has its eigenvalues in the convex region $\boldsymbol{D}$ if the LMI with A is solvable. Thus, it is true to say that the matrix A has all its eigenvalues in the LMI region $\left\{z \in \boldsymbol{C}: f_D(z) = [\alpha_{ij} + \beta_{ij} z + \beta_{ji} \bar{z}]_{1 \le i,j \le m} < 0\right\}$ if and only if there exists a symmetric P such that:

$$[\alpha_{ij} P + \beta_{ij} A^T P + \beta_{ji} P A]_{1 \le i,j \le m} < 0 \quad where \quad P > 0 \tag{3.30}$$

The region in which poles are located is an indication of transient performance specifications [33]. These can include rise time and settling time of a control system [31]. Also, it will keep the feedback gain at a reasonable value [34]. For more information see [31,40,41].

3.3 – Multi-Objective State Feedback

In 1963, [43] introduced multi-objective optimization in the form of a control problem. From this point onward, the controller design problem could be formulated as a multi-objective problem. What is a multi-objective problem? It is one in which there can be n optimized control specifications of f. The most basic form is

$$\min_{K} \left(f_1(K)\ f_2(K)\ \ldots .\ f_n(K)\right)^T$$

$$subject\ to\ K \in\ \Omega$$

Where Ω is the set of all controllers which internally stabilize the plant, P.

During the 1990's, researchers including Mahmoud Chilali, Pascal Gahinet, and Carsten Scherer worked on combining all of the different types of control problems. They explored the flexibility of these types of problems, and found that they could be combined in LMI form as a multi-objective optimization problem [36].

By formulating a multi-objective problem, many different performance criteria can be met including: control effort, output error, frequency response, rise time, settling time, and gain and phase margins. However, this does mean that the control objectives must trade-off their objectives to find one which satisfies all of them for a sub-optimal control. This creates another optimization problem when studying the relationships between these objectives. The H_∞ problem is essentially a frequency domain response which does not provide much control over transient behaviors [41]. The H_∞ norm bound ensures robust stability from perturbations, and the H_2 bound minimizes a guaranteed cost for the LQG problem. The pole placement requirements ensure adequate system damping and time response. All of these provide their own optimal controllers; however, when combined, they allow for a more desirable controller overall [44].

There are tradeoffs in performance when a problem is formulated multi-objectively. For example, the control effort will increase based on the expected placement of the closed loop poles [45]. The H_2/H_∞ problem guarantees that there will be robust stability while minimizing the H_2 norm performance measure [36].

As interior point methods became more fully developed, research began to use them to formulate a mixed objective convex problem over LMIs [46]. As research continued, it was determined that general quadratic synthesis procedures allowed the formulation of multi-objective output feedback control with LMI optimization. H_2 performance, H_∞performance, and regional pole constraints were among the types of constraints that could now be formulated into the problem [42]. However, with this technique, LMIs must all be formulated as the internally stabilizing controller, where the closed loop system must satisfy the quadratic Lyapunov function:

$$\min \mathrm{V}(\mathrm{x_{cl}}) = x_{cl}^T P x_{cl} \ , \quad P > 0$$

$$such\ that\ A_{cl}^T P + P A_{cl} < 0$$

where

- A_{cl} is the closed loop state matrix
- x_{cl} is the closed loop state vector

This assumption means that all of the constraints can be solved with the same Lyapunov function. Therefore, it is conservative in nature and may not find the most optimal controller. However, without this assumption, the multi-objective design becomes a system of bilinear matrix inequalities (BMIs). At this time, there are no reliable numerical ways to solve these problems [47, 48, 49]. Therefore, we proceed knowing that this conservatism is built into the problem.

It should be noted that there are two other potential ways to solve the multi-objective problem if one desires to explore other options more thoroughly:

1. An infinite dimensional convex optimization problem explained in detail in [50]. Although this can provide a better approximation, the technique increases the order of the controller.
2. Multi-objective genetic algorithms are a nondeterministic approach to the control formulation that is based off the artificial implementation of natural selection. Details on this technique can be seen in [36].

With a basic understanding of theory, it is now time to evaluate the multi-objective problem. The first objective is to evaluate what the transfer function of a multi-objective LTI state feedback equation would look like. The plant is $P(s)$ which is a given LTI system. Fig. 3.3 gives the state feedback representation of the problem.

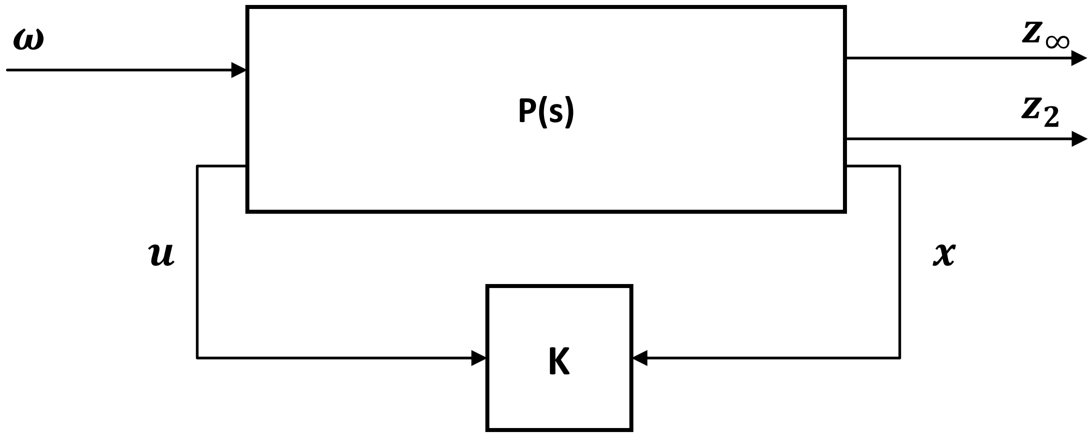

Fig. 3.3 – State Feedback Control Diagram

The following are the state equations for this system:

$$\begin{aligned} \dot{x} &= Ax + B_1\omega + B_2u \\ z_\infty &= C_1x + D_{11}\omega + D_{12}u \\ z_2 &= C_2x + D_{22}u \\ y &= C_yx + D_{y1}\omega + D_{y2}u \end{aligned} \tag{3.31}$$

where

- **x** is the system state
- **u** is the control
- ω is a disturbance
- $\boldsymbol{z}_\infty$ and $\boldsymbol{z}_2$ are for the $\mathbf{H_2/H_\infty}$ problems
- **y** is the output

It must be assumed that the ω values are the same in each equation in order to find a convex approximation [51]. The goal is to design closed loop transfer functions from ω to z_∞ and $z_2$with a state-feedback law of $u = Kx$ such that [34]:

- The RMS gain of $\|T_\infty\| < \gamma_0$ where $\gamma_0 > 0$
- The $\|T_2\| < \upsilon_0$ where $\upsilon_0 > 0$
- $\alpha\|T_\infty\|^2 + \beta\|T_2\|^2$ is minimized
- The closed loop poles lie in the left-half plane defined by D

The closed loop state equations are:

$$\begin{aligned} \dot{x} &= (A + B_2K)x + B_1\omega \\ z_\infty &= (C_1 + D_{12}K)x + D_{11}\omega \\ z_2 &= (C_2 + D_{22}K)x \\ y &= C_yx + D_{y1}\omega + D_{y2}u \end{aligned} \tag{3.32}$$

H_∞ Controller:

$$\begin{pmatrix} {A_{cl}}^T P_\infty + P_\infty A_{cl} & B_{cl} & P_\infty C_{cl\infty} \\ B_{cl}^T & I & D_{cl\infty}^T \\ C_{cl\infty}P_\infty & D_{cl\infty} & -\gamma_\infty^2 I \end{pmatrix} < 0 \qquad P_\infty > 0 \tag{3.33}$$

H_2 Controller:

$$\begin{pmatrix} A_{cl}P_2 + P_2A_{cl}^T & B_{cl} \\ B_{cl}^T & -I \end{pmatrix} < 0 \qquad P_2 > 0 \tag{3.34}$$

$$\begin{pmatrix} Q_2 & C_{cl}P_2 \\ P_2C_{cl}^T & P_2 \end{pmatrix} > 0$$

Pole Placement Control:

$$\begin{gathered} \left[\alpha_{ij}P_D + \beta_{ij}A_{cl}^T P_D + \beta_{ji}P_D A_{cl}\right]_{1 \le i,j \le m} < 0 \\ Trace(Q) < \upsilon_0^2 \qquad P_D > 0 \\ \gamma^2 < \gamma_0^2 \end{gathered} \tag{3.35}$$

The need for $\gamma^2 < \gamma_0^2$ is explained in detail in [31, 35].

The combination works because it is decided that a single Lyapunov matrix must be found such that:

$$P = P_D = P_\infty = P_2 > 0 \tag{3.36}$$

This makes the problem suboptimal. Additionally, the system formulation is still not yet convex because $A_{cl}P$ is a product of KP. Therefore, two substitutions must be made for this to become a convex problem.

1. $X^{-1} = P$
2. $L = KX$

Now, the next equations demonstrate the convex optimization problem which occurs during the multi-objective LMI procedure:

$$\min(\alpha\gamma^2 + \beta trace(Q))\ over\ L, X, Q, \gamma^2\ such\ that$$

$$\begin{pmatrix} AX + XA^T + B_2L + L^TB_2^T & B_1 & XC_1^T + X^TD_{12}^T \\ B_1^T & -\gamma I & D_{11}^T \\ C_1X + D_{12}L & D_{11} & -\gamma I \end{pmatrix} < 0$$

$$\begin{pmatrix} Q & C_2X + D_{22}L \\ XC_2^T + L^TD_{22}^T & X \end{pmatrix} > 0$$

$$\left[\alpha_{ij}X + \beta_{ij}(AX + B_2L) + \beta_{ji}(XA^T + L^TB_2^T)\right]_{1\le i,j\le m} < 0$$

$$trace(Q) < \nu_0^2$$

$$\gamma^2 < \gamma_0^2$$

*Note: that $A_{cl} = A + B_2K$ and $C_{cl2} = C_2 + D_{22}K$ were expanded for clarity.

Assuming that the above equations are feasible, the optimal solution is denoted by $(X^*, L^*, Q^*, \gamma^*)$. The corresponding state-feedback gain is given by

$$K^* = L^*(X^*)^{-1}$$

This gain guarantees the worst-case performances

$$\|T_{\infty}\|_{\infty} \leq \gamma^*$$

$$\|T_2\|_2 \leq \sqrt{\left(Trace(Q^*)\right)}$$

3.3.1 – Polytope Created

The polytope created for this thesis relies on this concept of multi-objective control because at each vertex, there is a multi-objective controller. The vertices of the polytope created are represented as the k^{th} system denoted by S_k has the form:

$$S_k = \begin{bmatrix} A_k & B_{k1} & B_{k2} \\ C_1 & D_{k11} & D_{k12} \\ C_{k2} & 0 & D_{k22} \\ C_{ky} & D_{ky1} & D_{ky2} \end{bmatrix} \tag{3.37}$$

The convex combination of the systems is given by,

$$S\{S_1, S_2, \dots S_k\} = \left\{ \sum_{i=1}^{k} \alpha_i S_i : \sum_{i} \alpha_i = 1, \alpha_i \geq 0 \right\} \tag{3.38}$$

The non-negative numbers $\alpha_1, \alpha_2, \dots, \alpha_k$ are the polytopic coordinates of S. Many of the convex combinations in (3.38) have simple explanations. If S_1 is the base case and S_2 is an outage of a tie-line, then $\alpha S_1 + (1-\alpha)S_2$ can be thought of as continuously increasing the impedance of the tie-line until it is open. This is how the boundaries of the polytope are formulated. In two dimensions, this polytope can be represented as seen in Fig. 3.3. The third vertex, S_3, is an increase in the load. Combinations of these three contingencies are contained within the polytope. Convexity will be addressed in Chapter 4. It should be noted that the polytope actually has many more dimensions because it grows by the size of the system each time a new vertex is added.

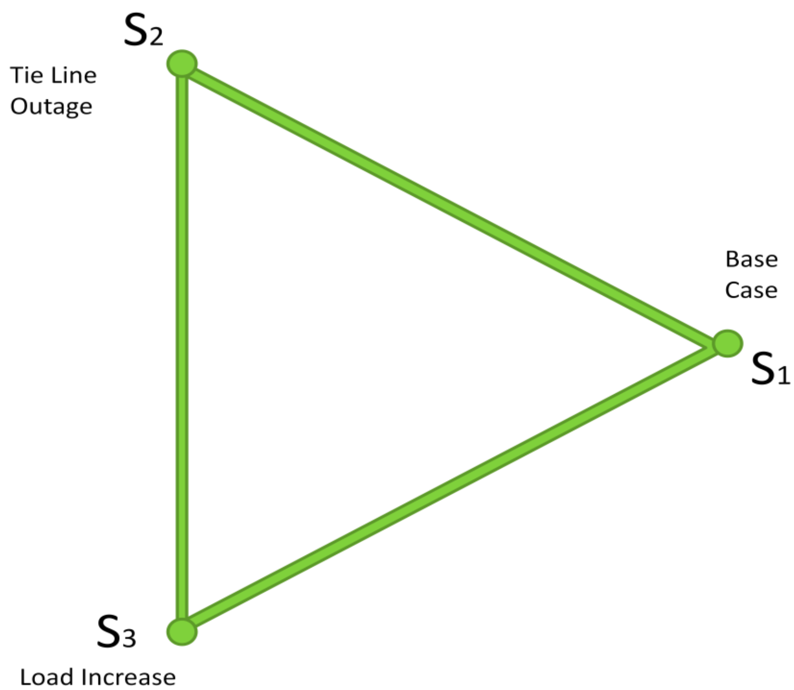

Fig. 3.4: Two dimensional representation of a polytope made of three contingency cases

By solving this set of polytopes using the Matlab Robust Control Toolbox, one single gain matrix, K, is found. The function needed is msfsyn. This K creates a controller which ensures that all of the criteria established in the formulation of the LMI are met. If any of the three contingencies were to occur, this control could damp the resulting inter-area oscillation. This is a huge improvement over the previous controllers which could only damp one inter-area oscillation at one frequency.

The work presented in this chapter provides an overview of H_2, H_∞, pole placement, and multi-objective control theory. This work was developed in some part because it was difficult to find all of these control concepts together in one source. I thought it would be beneficial to have all of this information in one location for future references. The LMI technique designs a robust controller. LMI systems have several advantages. Numerical solvers are readily available. Once a control problem has been formulated as an LMI, other LMI constraints can be added [52,53].

The H_2 LQG design parameters are tailored more towards measuring the control effort and providing disturbance rejection. The H_∞ analysis is used to evaluate how robust a system is when exposed to dynamic uncertainty [5]. For this reason, joining the two is a natural way to achieve a more robust response. The H_∞ problem can then minimize the maximum errors to provide better information for the H_2 problem.

Because the H_∞ control does minimize the maximum error and then take the norm of that minimized error and ensure that it is $< \gamma$, it is computationally and time intensive. Much iteration occurs before the optimization is through due to little change in the minimum value. Thus, it becomes difficult to do when the system becomes larger. In addition to the slow speed, the LMI formulation has the disadvantage that LMIs cannot be produced for a general class of problems. Each formulation much be done empirically [52]. Furthermore, the LMI formulation of a multi-objective problem constrains the optimality of the solution. The solution will be suboptimal.

While the Robust Control Toolbox provides a state-of-the-art LMI solver and is faster than solving a classical optimization problem, it is still extremely computationally intensive. MATLAB and those working with the robust control toolbox expect to see improvements in its speed and ability to handle more contingency cases. Even since I have been working on this problem, MATLAB has improved the toolbox by now allowing unlimited contingency cases. In previous versions, only eight were allowed. However, this does not reduce the computational complexity of the problem to be solved. This means, that another technique must be introduced to increase the size of the problem without increasing complexity.

Chapter 4 – Adaptive Control Technique

After introducing the complexity and issues associated with multi-objective state feedback control in Chapter 3, we will now evaluate a solution for those concerns. In order to create a more practical controller which encompasses more contingency cases, the computational complexity of the LMI polytopic synthesis must be decreased or circumvented.

In [16], Selective Modal Analysis (SMA) was used to reduce the system size. However, by doing so, they reduced control over some of the local modes because generators were dropped from the system model. Even with that loss of control, all of the local modes were damped by at least 7.5% which is perfectly acceptable. Additionally, the control algorithm proposed in [16] damped the inter-area modes by more than 15% which is an exceptional result. Despite these positive results, further reduction of complexity is desirable.

The MATLAB Robust Control Toolbox now allows for more contingencies, or equivalently, vertices, which means that the controller can handle more cases. However, because there is just one control to damp all of the oscillations caused by each case, the contingencies must be very similar in nature for the controller to be feasible [28].

One way to reduce the complexity of an individual polytope is to separate the contingencies into groups. These groups can vary in the number of cases they encompass. However, for this technique to be relevant, a controller which covers all of the contingencies that comprise the individual polytopes must be infeasible. However, all of the cases must have the same base case, S_1. Having the same base case means that both the polytopes have the same system configuration before contingencies are applied. For example, cases $S_1, S_2, and\ S_3$ must be able to be solved for a controller, K_1. Additionally, cases $S_1, S_4, and\ S_5$ must be able to be solved for a different controller, K_2, because the contingencies represented in $S_4, and\ S_5$ are different from those in $S_2, and\ S_3$. A two-dimensional image of what the two different polytopes are for five contingency cases is shown in Fig 4.1. There are actually many dimensions to each polytope.

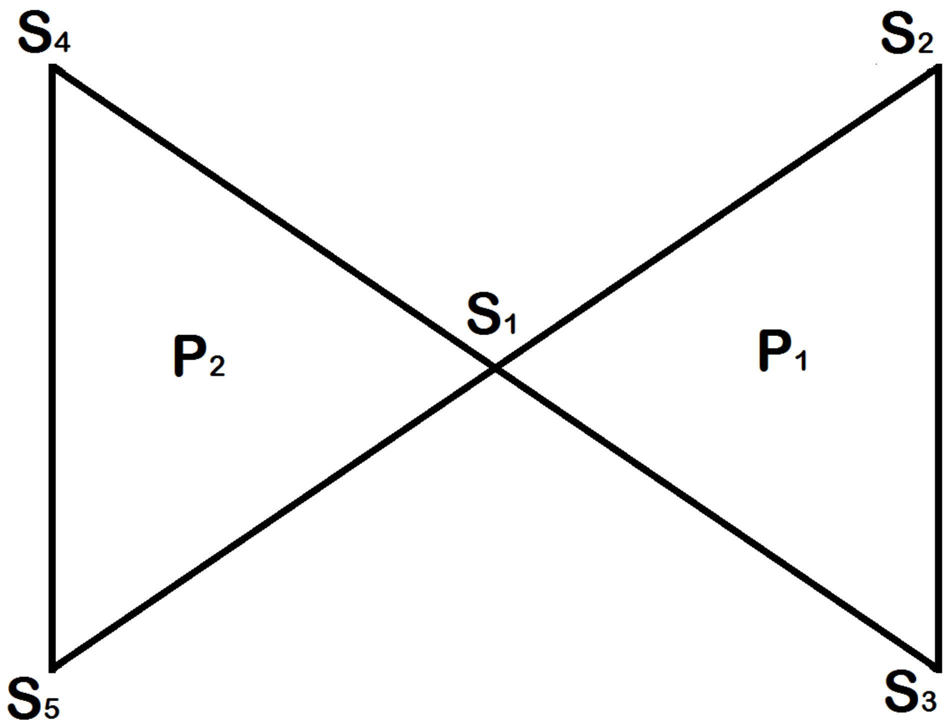

Fig. 4.1: Two polytope example with one common base case.

4.1 – Mathematical Background

To understand the algorithm presented, a very basic understanding of convexity and convex combinations is necessary.

4.1.1 – Convex Combinations

First, we will begin with the definition of a convex set as defined in [53]:

Given that V is a linear space, and a subset $C \subset V$ is convex if the line segment between any two points in C lies in C, *i.e.*, if for any $x_1, x_2 \in C$ and any θ with $0 \leq \theta \leq 1$, we have

$$\theta x_1 + (1 - \theta) x_2 \in C \tag{4.1}$$

In more basic terms, a given set is convex if every point in the set can be seen by every other point. There should be a straight line in between them. All affine points are also convex. The set of convex combinations is shown in the shaded purple region of Fig. 4.2.

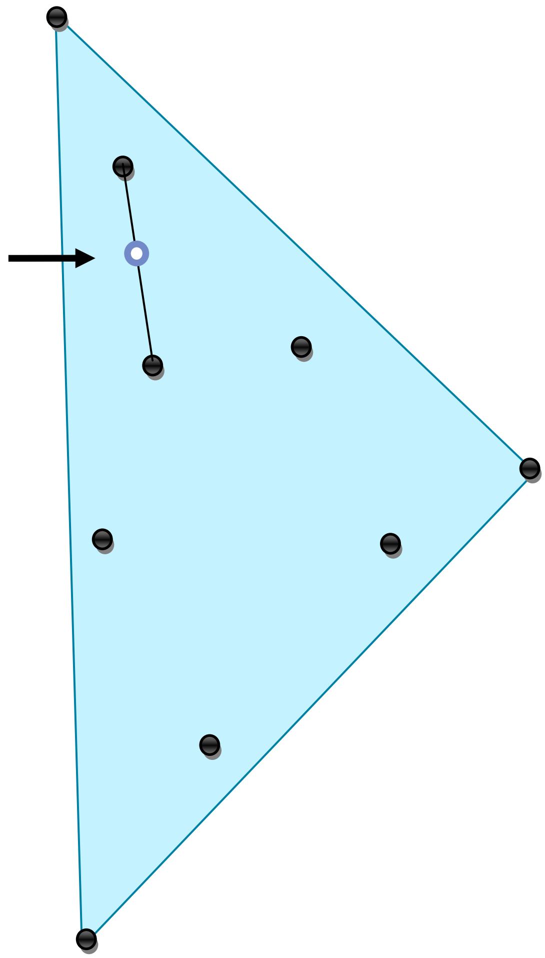

Fig. 4.2 – Convex Set

It is formed by varying the values of θ. The following is the mathematical representation of a convex combination. There are $\theta_i's$ which satisfy

$$\sum_{i=1}^{k} \theta_i = 1 \,, \qquad \theta_i \geq 0$$

Where

$x_1, x_2, \ldots \in C$, where $C \subseteq \boldsymbol{R}^n$ is convex, then:

$$\sum_{i=1}^{k} x_i \theta_i \in C$$

All of these black points represent points in the set. This shape represents the smallest convex set which can contain all of these black points. The hollow blue dot is in the convex set found on the line between two points in the convex set.

Solving for the convex combination of points provides the convex hull of the system. Additionally, if a set is convex, the convex hull is equivalent to the entire set.

This formulation is similar to the definition of the span of a set; however, it is different because of the demand that $\sum_{i=1}^{k} \theta_i = 1$. This criterion forces us to project inward from a set of points, rather than outward as could be done in a span [55].

For LMIs, it is necessary to determine the feasibility of the problem. This means that the following must be true for the optimization problem to be feasible.

$$x \in \boldsymbol{R}^n \ (or\ matrices\ X_1, \ldots X_K) satisfying$$

$$A(x) < B(x)$$

4.2 – Algorithm

With the concept of a convex combination in mind, the algorithm developed is subsequently explained.

1. At least two polytopes must be formed with individual contingency cases. Each polytope has an individual controller, $K_1 and\ K_2$, respectively. Additionally, one control, $K,$ cannot stabilize all of the cases.
2. The matrix Φ is derived by transforming the time invariant closed loop state matrix, A, into a discretized matrix with a sample time T_S.
3. This matrix is then used to calculate values for α recursively

Each vertex of the system represents a contingency, and each polytope has different cases. The LMI control was initially tested for the entire system and was found to be infeasible. After $1 \ldots n$ polytopes were solved for their individual optimal controls, the following convex combination can be solved –

$$\mathrm{x}(m) = \sum_{i=1}^{n} \Phi_i x_i(m-1)\alpha_i \tag{4.2}$$

$$\sum_{i=1}^{n} \alpha_i = 1 \tag{4.3}$$

$$\alpha_i \geq 1 \tag{4.4}$$

When expanded, (4.2) looks like (4.5).

$$x(m) = \Phi_1 x_1(m-1)\alpha_1 + \Phi_2 x_2(m-1)\alpha_2 + \Phi_3 x_3(m-1)\alpha_3 \tag{4.5}$$

where

- m is the number of samples taken
- $x(m)$ is the convex combination of the variables.
    - $x(m)$ has the dimension $states\ x\ 1$ for this example for each individual value of m. This is the input matrix for which we have to identify a controller. This is why it is only $system\ x\ 1$ and does not depend on the number of vertices of the polytope. The elements of x are the δ and ω values of the generators in the system.
- n is the number of vertices in a polytope.
    - In the following example, $n = 3$ because each polytope is composed of three vertices.
- Φ_i is the matrix made from each A_i matrix.
    - It will have the dimensions $states\ x\ states$ because it is derived from the A matrix.

- $x_i(m-1)$ is the matrix of previous values of $x(m)$. This formulation allows the problem to be solved recursively.
    - It will have the dimension $states\ x\ vertices$ because it is left multiplied with the matrix Φ_i which has the dimension $states\ x\ states$. It is right multiplied with the $vertices\ x\ 1$ vector of $\alpha's$ on the right. Similarly, the elements of x are composed of the δ and ω values of the generators in the system.
- α_i are the scalar values associated with each polytope.
    - For this problem, we utilize the vector of $\alpha_i's$. It has the dimension $vertices\ x\ 1$.

The values of α_i can be solved for using the pseudo-inverse as illustrated in (4.6).

$$\alpha_i = \left(\left(\Phi_i x(m-1)\right)^T \left(\Phi_i x(m-1)\right)\right)^{-1} \left(\Phi_i x(m-1)\right)^T x(m) \tag{4.6}$$

Equation (4.2) implies that if the contingency can be damped with the control provided by the i^{th} polytope, then α will converge to a fixed value for that polytope and diverge for all other polytopes.

In the most basic sense, the goal is to determine if the vector input signal is an operating point which is encompassed in either of the polytopes. This is a heuristic way of determining whether this point is within the convex hull produced by the polytope. If the $\alpha's$ indicate steady-state stability, this point forms a convex combination and is inside of the set. However, if the $\alpha's$ do not form a set with any of the polytopes developed, there is no previously designed control which can damp the oscillation. This will be explained in further detail in the example provided in Chapter 5.4.

4.3 – Conclusions on Adaptive Control

It should be noted that this control technique is not quite “adaptive” in the control sense. An adaptive controller is one which senses change and then readjusts the gain matrix, K, for that change. This control algorithm does evaluate the new system inputs, but is somewhat analogous to a gain scheduling algorithm, except it schedules the control. In a gain scheduling algorithm, a non-linear system is controlled with a set of linear controllers that satisfactorily stabilizes the system at various operating points. Observer variables determine the operating region of the system and then apply the appropriate linear controller. Similarly, this algorithm determines what control needs to be used to maintain stability. However, it is “adaptive” in that it changes the control applied based on the system conditions.

This is an interesting problem to evaluate, but it is limited by the number of polytopes that can be created. Can the power systems world be covered by polytopes with previously solved gains that damp a small number of conveniently planned contingencies? No, it cannot be. Moreover, this heuristic technique is prone to possible numerical errors. There could be a boundary condition of the convex set which is not observed when calculating the $\alpha's$. For the current design, this is not an issue because we have ensured that the polytope formed includes the boundaries. This could become an issue if contingency cases were chosen such that they were outside of the bounds of the problems. Despite the drawbacks, this concept may be able to be applied to a better posed or completely new problem in the future.

Chapter 5 – Problem Formulation Testing and Results

In this chapter, the theory discussed previously is tested in a small power system. First, the power system being tested needed to be developed. This is explained in the first section. The mathematical concepts behind the placement of the HVDC line are in this section as well. Next, the contingency cases are explained, followed by the application of the LMI control. The adaptive control technique is described after that along with results.

5.1 – Information on the developed system

The test system was developed by taking the IEEE 16 Machine Model system and dividing it into the New England portion. The entire 16 machine model can be found in [17]. This smaller model has eight classically modeled generators and 15 buses with one HVDC line. The generators are classically modeled with the rotor angle and generator speeds. The system will be discussed in further detail in the following sections.

5.1.1 – Basic Mathematical Concepts

5.1.1.1 – State space system – provided by LF of PSTV3

Before the state space system can be determined, the load flow must be performed. For this work, the Graham Rogers PSTV3 MATLAB Suite was used. It utilizes a Newton-Raphson algorithm to solve for the load flow. Next, it is desirable to evaluate the small signal stability. Small signal stability is the stability of an operating point of a dynamic system when perturbed with small disturbances. The system behavior in the small frequency range evaluated here is generally expressed as a set of non-linear differential and algebraic equations. These algebraic equations come from the stator current equations [2]. The initial operating points are obtained by substituting the algebraic variables into the differential equations. Then, the set of equations is linearized about an equilibrium point. More information on this can be found in [2, 10].

Because this is a small signal analysis, the state space equations are an essential part of analyzing a power system. There are several ways to linearize a system, including using Newton's method and calculating the Jacobian matrix or using the small perturbations method and calculating manually. For this thesis, the PSTV3 Suite was used to find the state matrices by numerically perturbing each state of the model. Next, the program took the change (or difference) in the state and divided it by the magnitude of the perturbation. When the perturbed values return to equilibrium, the new values are returned to their initial condition. This process is then repeated, and thus provides the generic linear time invariant equations expressed by (5.1).

$$\dot{x}(t) = Ax(t) + Bu(t) \qquad (5.1)$$
$$y(t) = Cx(t) + Du(t)$$

where

- A is the state matrix. It is square and has the dimension equal to the number of states.
- B is the input matrix. It gives the proportion of the individual inputs that are applied to each state equation.
- C is the output matrix.
- D is the feed forward matrix.
- $x(t)$ is the state vector.
- $u(t)$ is the input vector.
- $y(t)$ is the output vector.

5.1.1.2 – Eigenvalues and what they indicate

Whether real parts of all eigenvalues in a system are negative is important. When they are, transients in a linear dynamic system decay over time. A stable system is one in which all transients decay. An unstable system is one in which one or more transients grow. This is a problem for power systems because when unstable, they will not operate properly. However, because power systems are nonlinear, a linear system model must be created. A linearized model may have a complex eigenvalue with a positive real component. When this happens, system oscillations of constant amplitude can occur, subject to limitation by the system's nonlinearity. The system, though compromised, can remain in operation for at least a while.

However, a growing oscillation can result in system collapse and failure. The system is threatened in either case.

At a basic level, the first step made towards controlling the system needs to be evaluating the role each generator plays in each mode. The first step is looking at the solution to the state equation. This is evaluated by (5.2):

$$x = \sum_{i=1}^{n} u_i \, z_i \tag{5.2}$$

where

- u_i is the ith right eigenvector of A
- z_i is the ith mode

One way to evaluate the roles of the generators is through modal analysis. When a state vector of a particular mode has a large entry corresponding to its right eigenvector, it should be evaluated [15, 2]. This eigenvector is commonly referred to as the mode shape. Another way of stating this is that a mode's right eigenvector provides the relative amplitude of the mode which is observed through the dynamic system states [17]. The largest amplitude of oscillation for a particular mode corresponds to the state with the largest eigenvector magnitude. When an eigenvector coefficient is zero for a certain state, the measurements of that state cannot see that mode [17]. The mode shapes can determine coherent machine groups in multi-machine systems [2]. The i^{th} eigenvalue, i^{th} left eigenvector, and system input define the i^{th} mode as a scalar function of time. Each mode satisfies the linear differential equation in (5.3)

$$\frac{dz_i}{dt} = \lambda_i z_i + v_i B u \tag{5.3}$$

where

- λ_i is the i^{th} eigenvalue of A
- v_i is the i^{th} left eigenvector of A

The eigenvalue of the A matrix can be found by solving (5.4):

$$\det(A - \lambda I) = 0 \tag{5.4}$$

Additionally, the ith right eigenvector satisfies (5.5)

$$Au_i = \lambda_i u_i \tag{5.5}$$

The ith left eigenvector satisfies (5.6)

$$v_i A = \lambda_i v_i \tag{5.6}$$

The eigenvalue of a mode can be represented as (5.7):

$$\lambda = -\zeta\omega_n \pm j\omega_d = -\sigma \pm j\omega_d \tag{5.7}$$

where

- ζ is the damping ratio
- $\omega_n = |\lambda|$ is the undamped natural frequency and is an indication of rise time
- ω_d is the damped natural frequency
- σ is the real part of the pole

The damping ratio and frequency of oscillation in Hertz can be provided by (5.8)- (5.9):

$$\zeta = \frac{\sigma}{\omega_n} \tag{5.8}$$

$$f = \frac{\omega}{2\pi} \tag{5.9}$$

When the damping ratio is positive, there is positive damping. It should be noted that oscillations in power systems do not normally require heavy damping, but that with the added system stresses of today's system, it is desirable to have more than 5% damping [17].

5.1.2.2 – Participation factors of speeds

Before applying any type of control, the participation factors of the rotor speeds are evaluated. The rotor speed can also be seen by evaluating what frequency is closest to zero. This is a good indication of the effectiveness of the control because it shows what generators will be most affected by the control.

The participation factor is an indication of what j^{th} generators should have control applied to them such that i^{th} inter-area oscillation is damped. Equation (5.10) provides the mathematical representation of a participation factor is

$$P_{ji} = v_j(i)u_j(i) \tag{5.10}$$

where

- $u_j(i)$ is the i^{th} right eigenvector of A
- $v_j(i)$ is the i^{th} left eigenvector of A

They provide the sensitivity of an eigenvalue to a change in diagonal elements in the state matrix which is helpful because we want to affect the least damped modes. The speed of the rotors is chosen because it is indicative of adding damping to the generator shaft [17].

If a participation factor for a generator is positive, adding damping at that generator increases the damping of that mode. If a participation factor for a particular generator is negative, adding damping at that generator will decrease the damping of the mode. When the participation factor is zero, there is no effect on the mode [17].

5.1.2.3 – Compass plot of rotor angles

The next way to determine the effectiveness of controls on inter-area oscillations is to look at a compass plot of the rotor angle terms in the state matrix, A. This right eigenvector is used to evaluate the state changes that occur when that mode of oscillation is excited. Therefore, the plot will show the modes oscillating against one another. It is an indication of the ability to monitor the mode from particular states, but it does not necessarily indicate if they are good for controlling them. This is why the participation factor and compass plot are used together [17].

5.1.1.4 – Controllability and Observability

The controllability of a system is how a mode will respond when the inputs are perturbed. When a mode responds to an input change, the mode is controllable through that input.

The observability of a system describes how each mode is seen in the system outputs. When a mode is seen by a measurement at the system output, the system is called observable in that output. There are several tests to evaluate the observability of the system. Controllability and observability are dual notions of the system [21]. These concepts can be studied in more detail in [46, 21].

5.1.1.4 – Stabilizability and Detectability

A system is stabilizable when there is a state feedback which makes the closed loop state matrix, $A + BK$, stable. A system is stabilizable if all of the positive real eigenvalues are controllable as determined through the Popov Belevitch Hautus Eigenvector Test.

A system is detectable if there is a gain matrix which provides a closed loop stable gain matrix of $A + GC$. The system is detectable of the positive real eigenvalues if the unobservable modes are stable. Stabilizability and detectability are dual notions, similar to those of controllability and observability [17].

5.1.2 – Example System Information

The system explained in the beginning of Section 5.1 can now be explained in its mathematical terms. First, the load flow of the system was run for the base case without a DC line. The following sections show the testing which determined the placement of the DC line.

5.1.2.1 – Eigenvalues of example system

First, given that the system is an eight generator system without a DC line, the state matrix, A will have the size, $14x14$. This is because one of the generators is the slack generator. The eigenvalues, damping, and frequencies of the 14 states are given in Table 5.1.

Mode #	**Eigenvalue**	**Damping**	**Frequency**
1	*-0.0713 - 2.9815i*	*0.0239*	*0.4745*
2	*-0.0713 + 2.9815i*	*0.0239*	*0.4745*
3	*-0.1035 - 4.1423i*	*0.025*	*0.6593*
4	*-0.1035 + 4.1423i*	*0.025*	*0.6593*
5	*-0.0939 - 4.7523i*	*0.0197*	*0.7564*
6	*-0.0939 + 4.7523i*	*0.0197*	*0.7564*
7	*-0.0711 - 5.7432i*	*0.0124*	*0.9141*
8	*-0.0711 + 5.7432i*	*0.0124*	*0.9141*
9	-0.0774 - 6.1407i	0.0126	0.9773
10	-0.0774 + 6.1407i	0.0126	0.9773
11	-0.0963 - 6.2692i	0.0154	0.9978
12	-0.0963 + 6.2692i	0.0154	0.9978
13	-0.0790 -10.0397i	0.0079	1.5979
14	-0.0790 +10.0397i	0.0079	1.5979

Table 5.1 – Eigenvalues, damping ratio, and frequencies for system without controller

This table provides insight into what eigenvalues are particularly poorly damped and what frequencies they are. The frequencies which are in italics and are underlined are the ones that need to be watched the most closely.

5.1.2.2 – Compass plot of rotor angles

Generator 1 has the lowest frequency so we will check the compass plot of it first in Fig. 5.1.

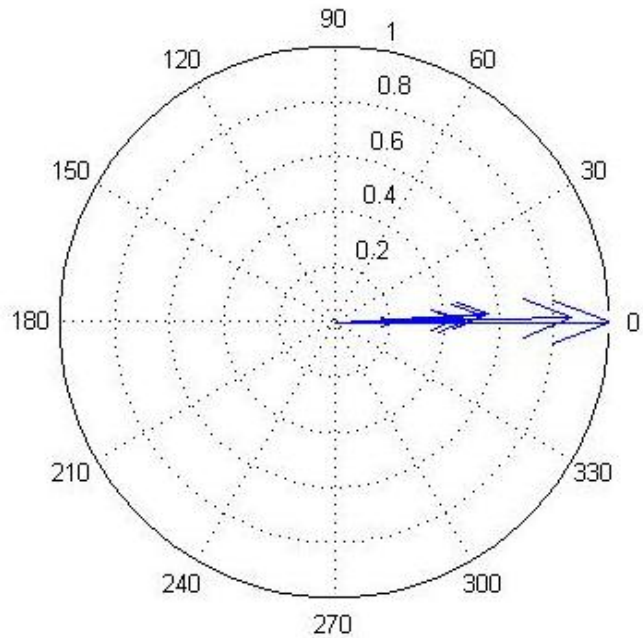

Fig. 5.1 – This graph indicates that there are no modes oscillating against each other. This means that this is not an inter-area mode even though it is at a low frequency.

Because this plot indicates that Mode 1 is not an inter-area oscillation, Mode 3 is tested. The Fig. 5.2 shows that Mode 3 has an inter-area oscillation.

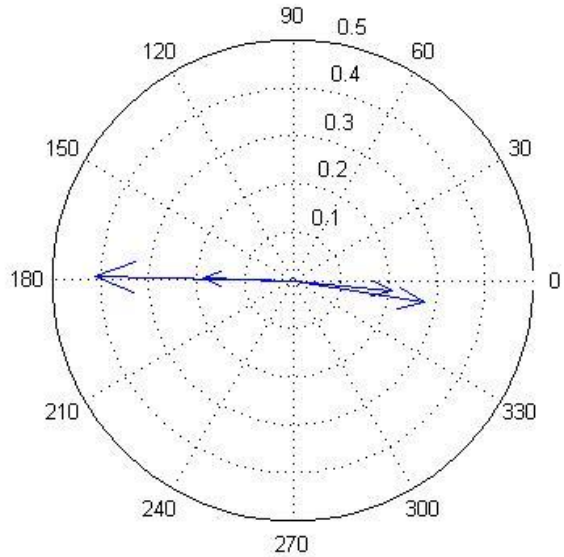

Fig. 5.2 – This shows that there are several modes oscillating against each other. This indicates an inter-area oscillation.

Because Fig. 5.2 shows that Mode 3 is an inter-area oscillation, the participation factors for that mode will be used to determine the placement for the HVDC line.

These plots were made with the command: compass(u(ang_idx,3)).

5.1.2.3 – Participation factors of speeds

Because the participation factors provide the sensitivity of an eigenvalue to a change in diagonal elements in the state matrix, we will calculate them for Mode 3. Fig. 5.3 shows the bar graph for the real part of the participation factors of the speed index for Mode 3. Note that Generator 6 was omitted because it is the slack bus.

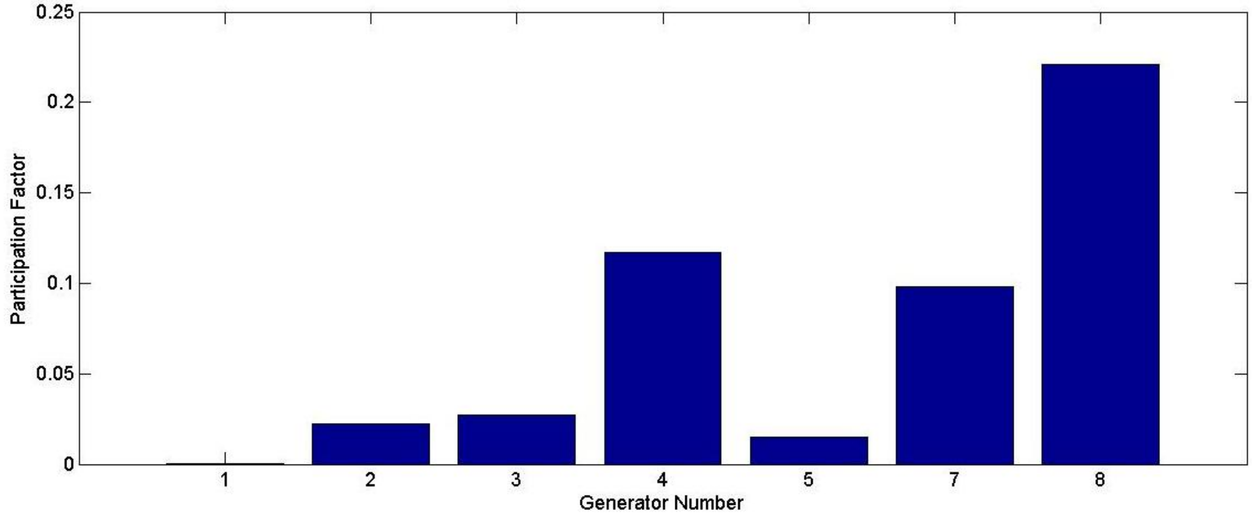

Fig. 5.3 - A bar graph of the participation factors for Mode 3

Fig. 5.3 has the highest participation factors for Generator 4 and 8. This means that to most effectively damp the inter-area Mode 3, it would be best to place the DC line between Generator 4 and 8.

This plot was made with the command: bar(real(p(spd_idx,3)).

5.1.2.4 – DC line placement and state matrices used in the H_2/H_∞ problem

With the following information, the system is now complete with the DC line between Generators 4-8. The DC line is indicated by the dashed line in Fig. 5.4.

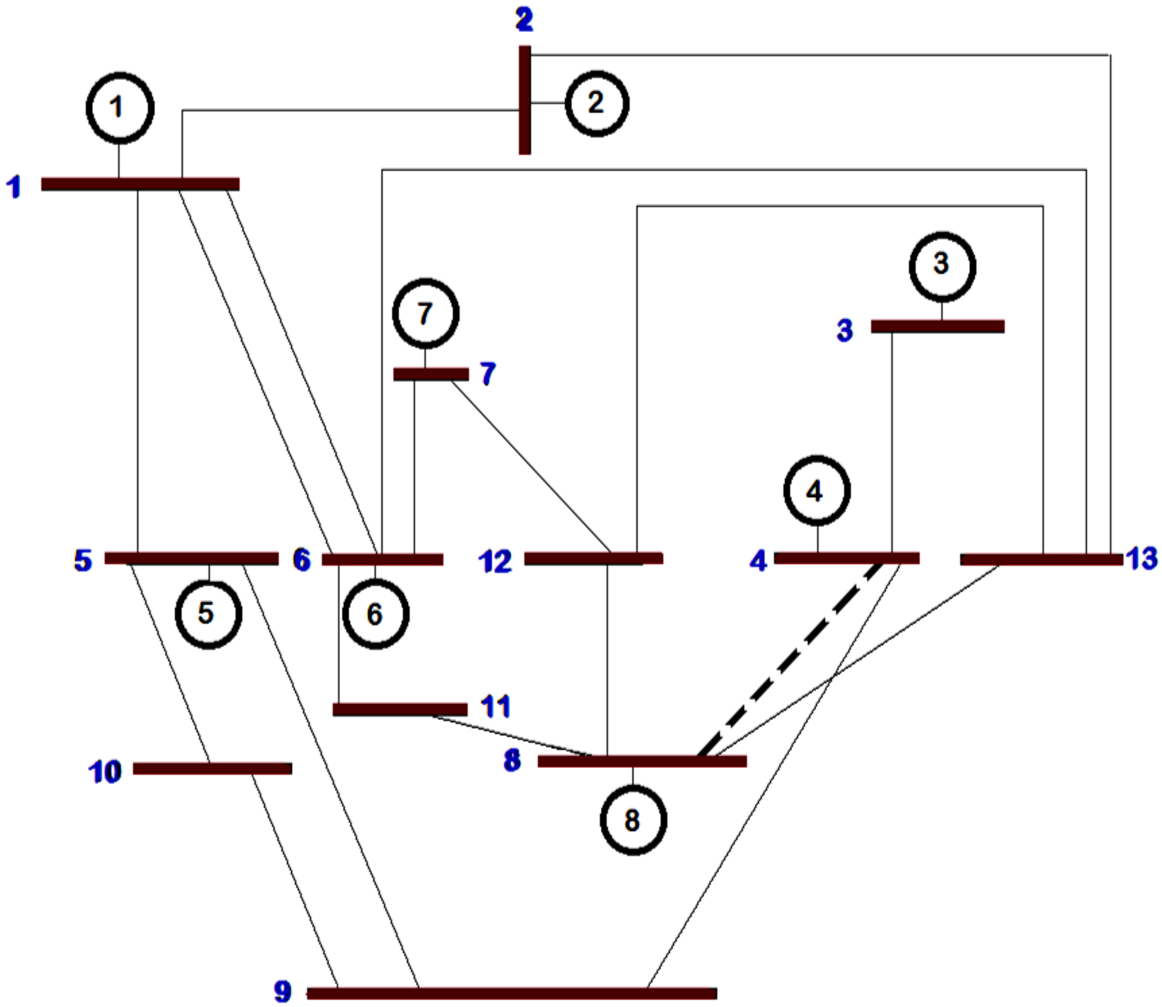

Fig. 5.4 – The example system with the DC line between 4-8

With the control now in place, the base case needs to be run for the system. The base case is the load flow solution when no contingencies have occurred.

The state space feedback representation of the system is given in Fig. 5.5 [47]. To see Fig. 5.5 and the state space formulas in (5.11) will help explain the sizes and meanings of the state matrices.

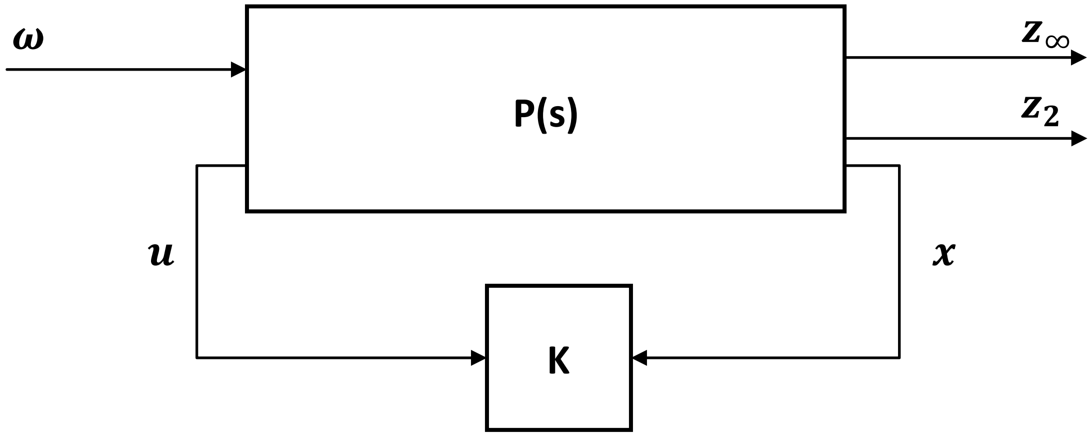

Fig. 5.5 - State Space Feedback Representation

The following (5.11) are the state equations.

$$\begin{aligned} \dot{x} &= Ax + B_1\omega + B_2u \\ z_\infty &= C_1x + D_{11}\omega + D_{12}u \\ z_2 &= C_2x + D_{22}u \\ y &= C_yx + D_{y1}\omega + D_{y2}u \end{aligned} \tag{5.11}$$

where

- **x** is the system state
- **u** is the control
- ω is a disturbance
- z_∞ and $z_2$are for the **H_2/H_∞** problems
- **y** is the output

The state space equations created from the PSTV3 Suite were of the following dimensions:

- $A \in \boldsymbol{R}^{15x15}$
  - This is because there were eight generators, but one was used as a slack generator. Therefore, there are seven angles and speeds associated with each generator which compose the A matrix. There is one control which accounts for the dimension of $15x15$.

- $B \in \boldsymbol{R}^{15x2}$
    - Respectively, the B_1 and B_2 matrices correspond to the disturbance and input vectors. Each matrix has the dimension $15x1$. It is a system requirement that the B matrix be the same length as the A matrix. It has mainly zeros except for the last row because that is where the control input is.
- $C \in \boldsymbol{R}^{8x15}$
    - The C_1 and C_2matrices correspond to the H_∞ and H_2 problems respectively. The matrix C_1 is actually a row vector which has the dimension $1x15$. It takes this size because the H_∞ norm ensures that the norm of those states is less than a particular value. The values in this vector are the output matrices values of the bus voltage angles. The matrix C_2 is the output matrix that corresponds to the generator speeds. It has the dimension $7x15$ and contains the identity matrix in order to control the frequency.
- $D \in \boldsymbol{R}^{2x8}$
    - The D matrix is actually composed of four different matrices.
        - D_{11} is $1x1$ scalar with the value of 1. This is because it has one element contributing to the disturbance. If $D_{11} = 0$ were the case, it would mean that there is no control for that particular disturbance.
        - D_{12} is a $1x1$ scalar with the value of 0. This is because it does not affect the H_∞ synthesis of the controller. The H_∞ synthesis is only concerned with tolerance to disturbances, thus input values are unnecessary.
        - D_{21} is a $7x1$ vector which must always be 0. The Robust Control Toolbox will not allow the problem to be started if the value is anything other than 0. This is because it D_{21} would feed forwarded errors into the H_2 optimization problem, and the system would become unstable.
        - D_{22} is a $7x1$ identity matrix. It feeds the input forward during the H_2 synthesis. Because this is just a vector, the top value is 1, and the rest are zeros.

The resulting system matrix for the base case has the dimension $28x18$. When formulated as an LMI vertex, an extra row and column are added so that the system matrix cannot be used accidentally. The Table 5.2 below shows the LMI system that is created. The first page shows matrices $A \; and \; B$. The second page of the Table 5.2 shows matrices $B \; and \; D$. It is evident that there is an extra row created with infinity at the bottom so that this system matrix cannot be used accidentally.

5.1.2.5 – The complete system matrix for the base case, i.e., the S_1 vertex.

Table 5.2 - The state matrices A and B are all denoted in the blocks.

0	0	0	0	0	0	376.9911	0	0	0	0	0	0	0	0	0	15
0	0	0	0	0	0	0	376.9911	0	0	0	0	0	0	0	0	0
0	0	0	0	0	0	0	0	376.9911	0	0	0	0	0	0	0	0
0	0	0	0	0	0	0	0	0	376.9911	0	0	0	0	0	0	0
0	0	0	0	0	0	0	0	0	0	376.9911	0	0	0	0	0	0
0	0	0	0	0	0	0	0	0	0	0	376.9911	0	0	0	0	0
0	0	0	0	0	0	0	0	0	0	0	0	376.9911	0	0	0	0
0.01826	0.00567	0.00539	0.064313	0.00455133	0.0050473	-0.19886	0	0	0	0	0	0	3.79E-05	0	0	0
-0.0908	0.01732	0.0008	0.00947	0.00303906	0.0041577	2.41E-12	-0.19022	2.41E-12	2.41E-12	2.41E-12	2.41E-12	2.41E-12	2.23E-05	0	0	0
0.01575	-0.0532	0.01249	0.004245	0.00205728	0.0030641	6.94E-13	6.94E-13	-0.21875	6.94E-13	6.94E-13	6.94E-13	6.94E-13	-6.55E-06	0	0	0
0.00024	0.0122	-0.0463	0.022444	0.00015192	0.0002444	1.73E-12	1.73E-12	1.73E-12	-0.10417	1.73E-12	1.73E-12	1.73E-12	-0.000274	0	0	0
-0.0026	0.00187	0.02406	-0.089139	0.00034386	0.0004663	-1.13E-12	-1.13E-12	-1.13E-12	-1.13E-12	-0.17857	-1.13E-12	-1.13E-12	-5.51E-05	0	0	0
0.01076	0.00812	0.00099	0.003068	-0.0864412	0.0336193	0	0	0	0	0	-0.15152	0	0.000241	0	0	0
0.00986	0.00732	0.00063	0.002315	0.01942786	-0.0644808	2.78E-12	2.78E-12	2.78E-12	2.78E-12	2.78E-12	2.78E-12	-0.375	0.000576	0	0	0
0	0	0	0	0	0	0	0	0	0	0	0	0	-43.6	43.6	43.6	0

Table 5.2 continued - The state matrices $B\ and\ D$ are denoted in the blocks.

-0.0125	-0.0015	-7E-5	0.152957	0.00658782	0.0078985	0	0	0	0	0	0	0	-4.91E-05	1	0	0
0	0	0	0	0	0	1	0	0	0	0	0	0	0	0	1	0
0	0	0	0	0	0	0	1	0	0	0	0	0	0	0	0	0
0	0	0	0	0	0	0	0	1	0	0	0	0	0	0	0	0
0	0	0	0	0	0	0	0	0	1	0	0	0	0	0	0	0
0	0	0	0	0	0	0	0	0	0	1	0	0	0	0	0	0
0	0	0	0	0	0	0	0	0	0	0	1	0	0	0	0	0
0	0	0	0	0	0	0	0	0	0	0	0	1	0	0	0	0
0	0	0	0	0	0	0	0	0	0	0	0	0	0	0	0	inf

5.2 – Contingencies Developed

The vertices of the system are composed of 5 different cases listed in Table 5.3.

Table 5.3 – System Contingencies

Vertex	**Contingency**
S_1	Base Case
S_2	Tie Line between 6-13 removed
S_3	Decrease load at Bus 9 by 8%, Increase load at bus 10 by 8%
S_4	Tie line between 12-13 removed
S_5	Decrease load at Bus 10 by 5%, Increase load at bus 9 by 5%

These particular contingencies were used because testing for the adaptive algorithm requires that not all of the contingencies be encompassed by one controller. This means that the eigenvalues of the different cases must be different enough from each other. If the eigenvalues are very similar, the controller will not need to work very hard to find a control to work for all of the contingencies. The loads are located at Buses 9 and 10. In order to create a divide of power flow, the impedance between those lines is the largest in the system. These cases were also chosen to start inter-area oscillations that would need to be damped. Additionally, these cases were also built to be the inverses of one another. This is to further ensure that one control cannot solve for all of the cases. It also allows for the added benefit of having two controllers which are more different from each other. This will help in the adaptive algorithm in Section 5.4. These cases were specifically chosen to create inter-area oscillations in the system that would need to be damped.

5.3 – Setting up the LMI regions

Feasibility is the first component of this system that must be tested. For the requirements of the adaptive control testing, the controller must not be able to damp all five contingencies with a single control, *i.e.*, there is no feasible solution to that problem. As expected, the control did not damp all five cases. Thus, the five contingencies were broken into two polytopes with the common base case, as shown in Section 4.1. However, for this system, the controller was split into different polytopes that what was shown in Section 4.1. The polytopes actually split into the groups seen in Fig. 5.6.

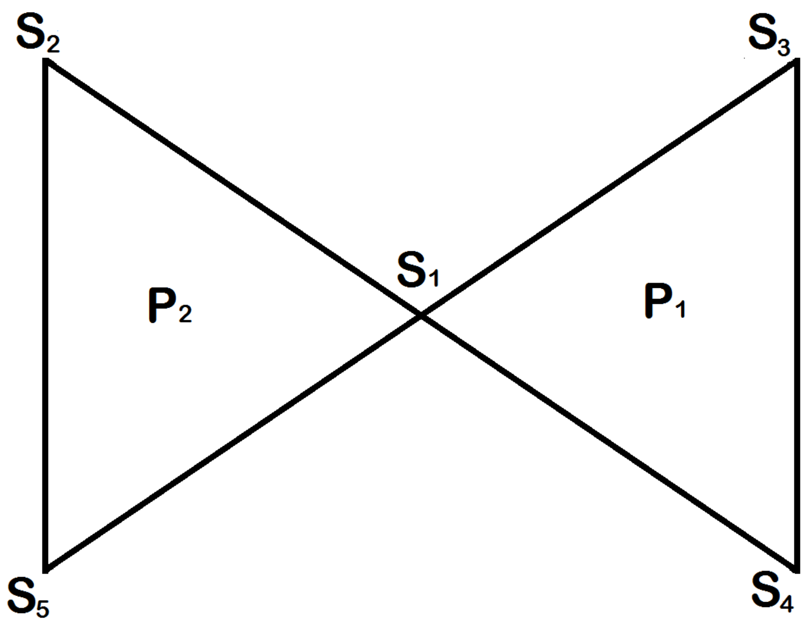

Fig. 5.6 - Polytopes created for this system

$$S_1, S_3, S_4 \in P_1$$

$$S_1, S_2, S_5 \in P_2$$

Now, it is necessary to solve for the controllers K_1 *and* K_2 for each polytope. There are several design specifications that surround this control choice.

The damping region chose was about 5%. This is much smaller than what is desirable, but with only one control in a relatively stressed, small system, it is satisfactory. The gain matrix, K_1, could provide damping up to about 10%. However, for future demonstrations, I decided they should keep the same damping region. The H_2/H_∞trade-off found that there was no consequential benefit to spending time finding the Pareto-optimal point. This may be more desirable if the system were larger, but under these circumstances, weighting their importance equally is also satisfactory.

5.3.1 – Results of LMI Testing

The following section presents the graphs of the LMI testing. The first graph, Fig. 5.7, shows the open and closed loop poles of P_1.

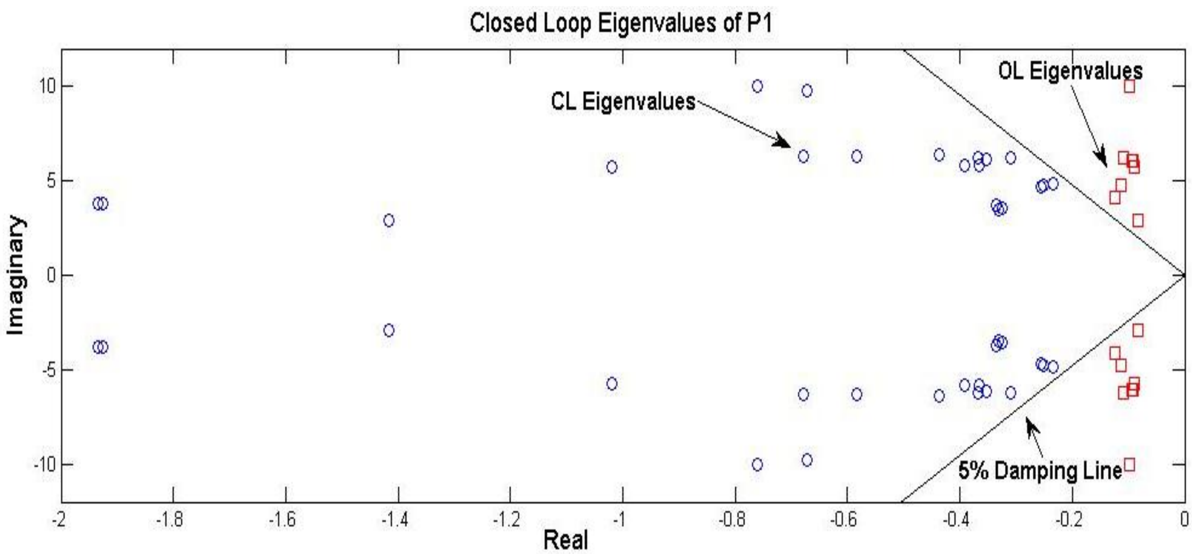

Fig. 5.7 – P1 Eigenvalues

In Fig. 5.8, there are the open and closed loop poles of P_2. The controller of the second polytope was able to make some of the poles move even further to the left. However, this was at the expense of controller cost.

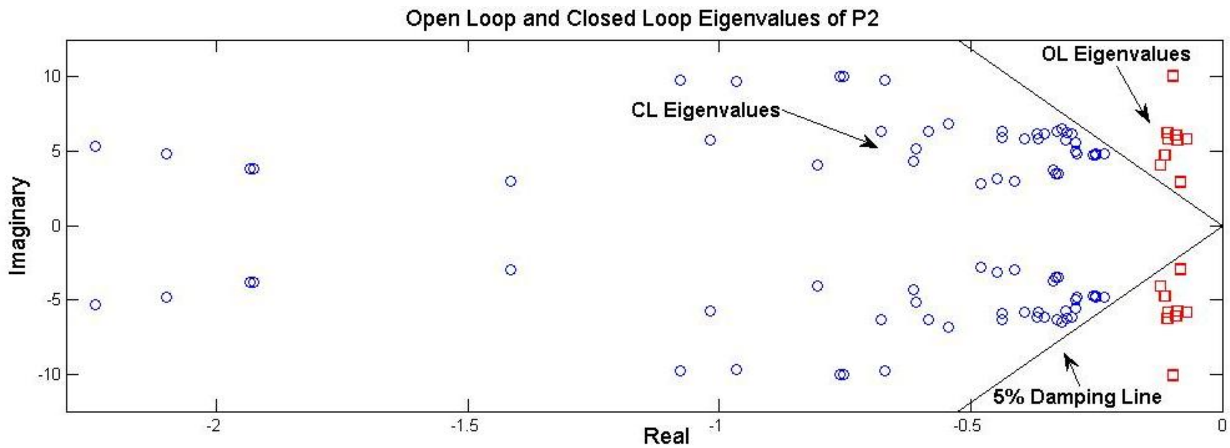

Fig. 5.8 – P2 Eigenvalues

Fig. 5.8 is the root locus plot for S_2 with K_1. The root locus plot shows the direction the poles are moving when the control is applied. They behave correctly in this example because all of them move to the left. This is seen in the Fig. 5.9 below. The squares represent the initial position of the eigenvalues whereas the circles denote their final position. From the figure, it becomes clear that all the eigenvalues have moved towards the left implying that the proposed adaptive selection method has been successful in choosing the correct control.

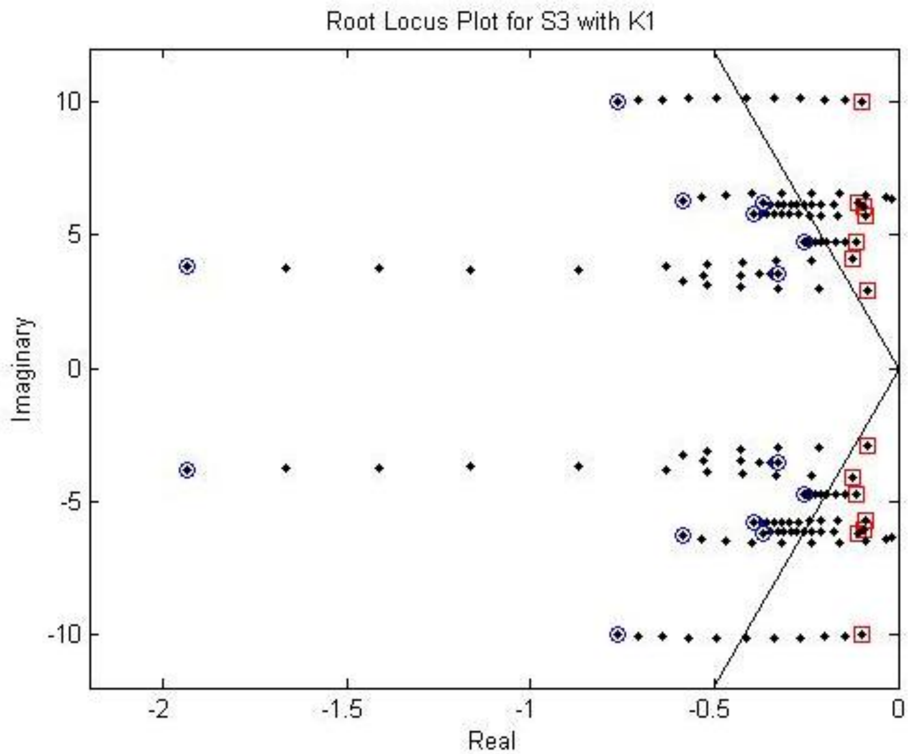

Fig. 5.9 – Root Locus of S3 with K1 applied

The following, Fig. 5.10, is a root locus plots for the vertex S_5 with K_2.

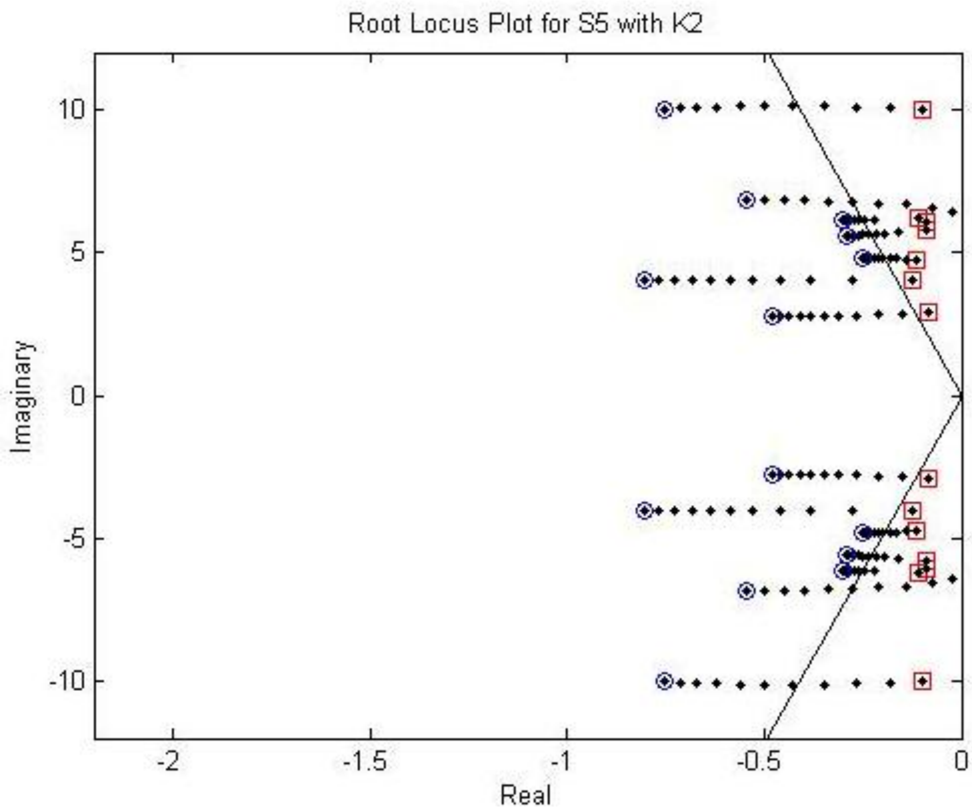

Fig. 5.10 – Root Locus of S5 with K2 Applied

Finally, there are several time domain plots which demonstrate the system response to a one degree step change in rotor angles at all of the generators. Fig 5.11 shows the open loop response.

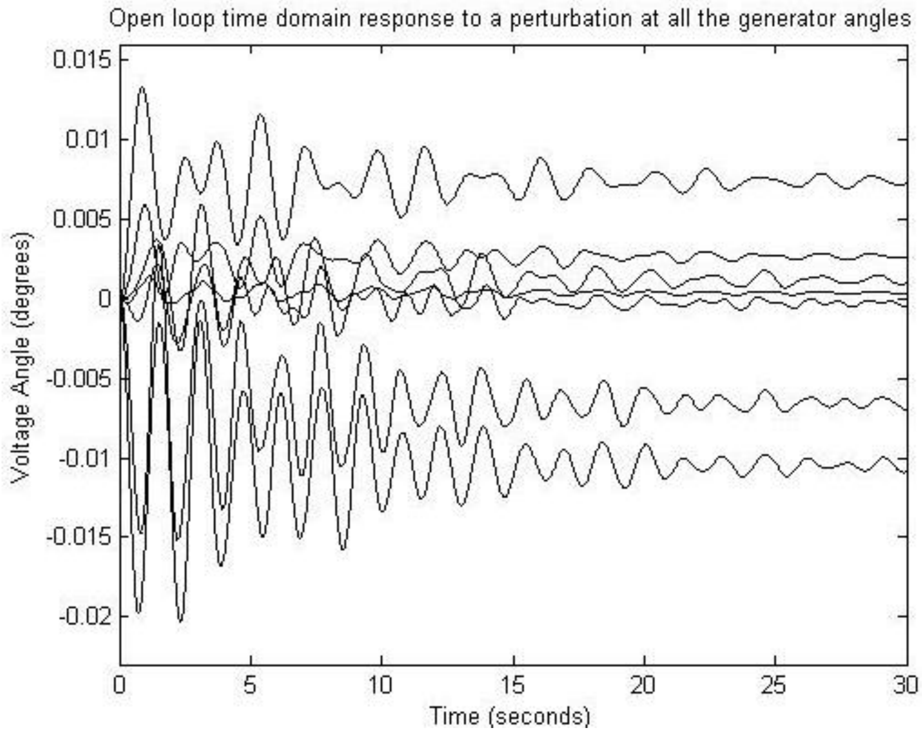

Fig. 5.11 – Time Domain Response of Step Input into S2

Fig. 5.12 shows the closed loop response. They are both on the same scale so that it is more obvious how much better the closed loop response is.

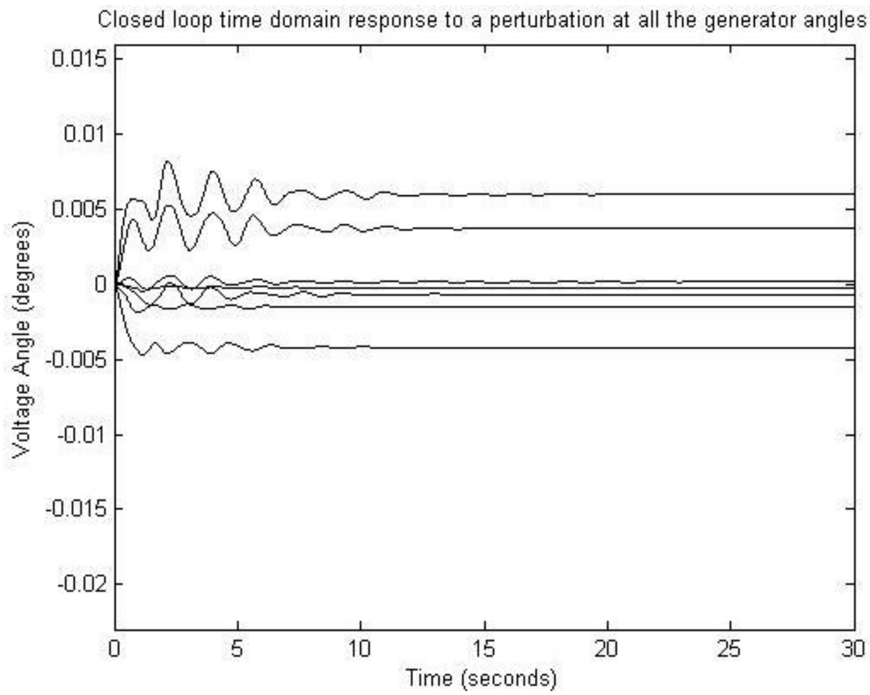

Fig. 5.12 – Time domain response of closed loop system when perturbed

The graphs indicate how well the control theory already in place could damp inter-area oscillations. It has proven successful in this small test system.

5.4 – Adaptive Control Technique

Now that the individual controllers have been identified, the adaptive control technique can be applied. For review of Chapter 4, the adaptive controller solves the convex combination given in (5.12)-(5.14) for α. This will determine if the system requires control that can be provided by a previously formed multi-objective controller. To do this, we further explore the constraints for satisfying a convex combination.

$$x(m) = \sum_{i=1}^{n} \Phi_i x_i(m-1)\alpha_i \tag{5.12}$$

$$\sum_{i=1}^{n} \alpha_i = 1 \tag{5.13}$$

$$\alpha_i \geq 1 \tag{5.14}$$

When expanded, (5.12) looks like (5.15).

$$x(m) = \Phi_1 x_1(m-1)\alpha_1 + \Phi_2 x_2(m-1)\alpha_2 + \Phi_3 x_3(m-1)\alpha_3 \tag{5.15}$$

where

- m is the number of samples taken
    - In the following example, $m = 30$ because, in theory, we would be evaluating one second's worth of data from a PMU at a rate of $\frac{1}{30}\ s^{-1}$.
- $x(m)$ is the convex combination of the variables.
    - $x(m)$ has the dimension $14x1$ for this example for each individual value of m. This is the input matrix for which we have to identify a controller. This is why it is only $14x1$ and does not depend on the number of vertices of the polytope.
- n is the number of vertices in a polytope.
    - In the following example, $n = 3$ because each polytope is composed of three vertices.
- Φ_i is the matrix made from each A_i matrix.
    - It will have the dimensions $14x14$ because it is derived from the A matrix.
- $x_i(m-1)$ is the matrix of previous values of $x(m)$. This formulation allows the problem to be solved recursively.
    - It will have the dimension $14x3$ because it is left multiplied with the matrix Φ_i which has the dimension $14x14$. It is right multiplied with the $3x1$ vector of $\alpha's$ on the right.
- α_i are the scalar values associated with each polytope.
    - For this problem, we utilize the vector of α_i's. It has the dimension 3x1.

The values of α_i can be solved for using the pseudo-inverse as illustrated in (5.16).

$$\alpha_i = \left(\left(\Phi_i x(m-1)\right)^T \left(\Phi_i x(m-1)\right)\right)^{-1} \left(\Phi_i x(m-1)\right)^T x(m) \tag{5.16}$$

Loosely speaking, if the α_i values meet the criterion listed in (5.12)-(5.14), the input vector of $x(m)$ forms a convex combination. This means that it is inside of the convex set defined by the formation of the polytope [53]. Therefore, the control developed for that polytope will work to damp the oscillation.

5.4.1 – Step by step methodology

The following is a breakdown of the steps performed in this algorithm. Note that the matrix dimensions are given for one sample. The matrices will grow as more samples are taken.

1. Find δ_i *and* ω_i values from each vertex of the system and order them as a $14x1$ vector that provides the initial value for $x_i(m-1)$.
2. Calculate Φ_i matrix values from each A_i matrix. It will have the dimensions $14x14$.
3. Find $F_i = \Phi_i x_i(m-1)$ matrix recursively. It will have the dimensions $14x3$.
4. Calculate the value of $\alpha' s$ to determine convexity heuristically.
    a. If $\alpha' s$ meets the criterion of (5.12)-(5.14), apply that polytopes controller to the system.
    b. If $\alpha' s$ does not meet the criterion of (5.12)-(5.14), check other polytopes for convexity.
        i. If $\alpha' s$ meets the criterion of (5.12)-(5.14), apply that polytope's controller to the system.
        ii. If there is no $\alpha' s$ for which the constraints are met, this method will be unable to supply a control for that particular contingency. The operating point of the system is outside of the bounds of the polytope.

5.4.2 – Algorithm Testing

The next step is to test this algorithm. To do so, I formed the polytopes previously seen in Fig. 5.6. The qualities of these polytopes are discussed in more detail in Section 5.2-5.3. The first polytope, P_1, was tested by assuming that the input vector, $x(m)$ is composed of equally weighted components of the vertices of P_1. This is shown in (5.17).

$$x(m) = \frac{1}{3}\big(x_1(m) + x_3(m) + x_4(m)\big) \tag{5.17}$$

Therefore, when the Φ_1, Φ_3, Φ_4 matrices are used to find F_1 and the $x(m)$ vector is defined by (5.17), the scalar values of $\alpha_1, \alpha_3, and, \alpha_4$ should be constant at the value of $1/3$. There could be a small initial perturbation as the recursive algorithm begins, but it should settle to a constant value quickly. The graph of the $\alpha's$ for this test is shown in Fig. 5.13. Note that if the input value $x(m)$ were weighted differently, but still such that the weights summed to one, the $\alpha's$ would take those values instead. This is more clearly explained in a modification to (5.17). $x(m) = .2\ x_1(m) +\ .2\, x_3(m) + .6\, x_4(m)$ the corresponding steady-state α vector would now be, $\alpha = [.2\ .2\ .6]'$.

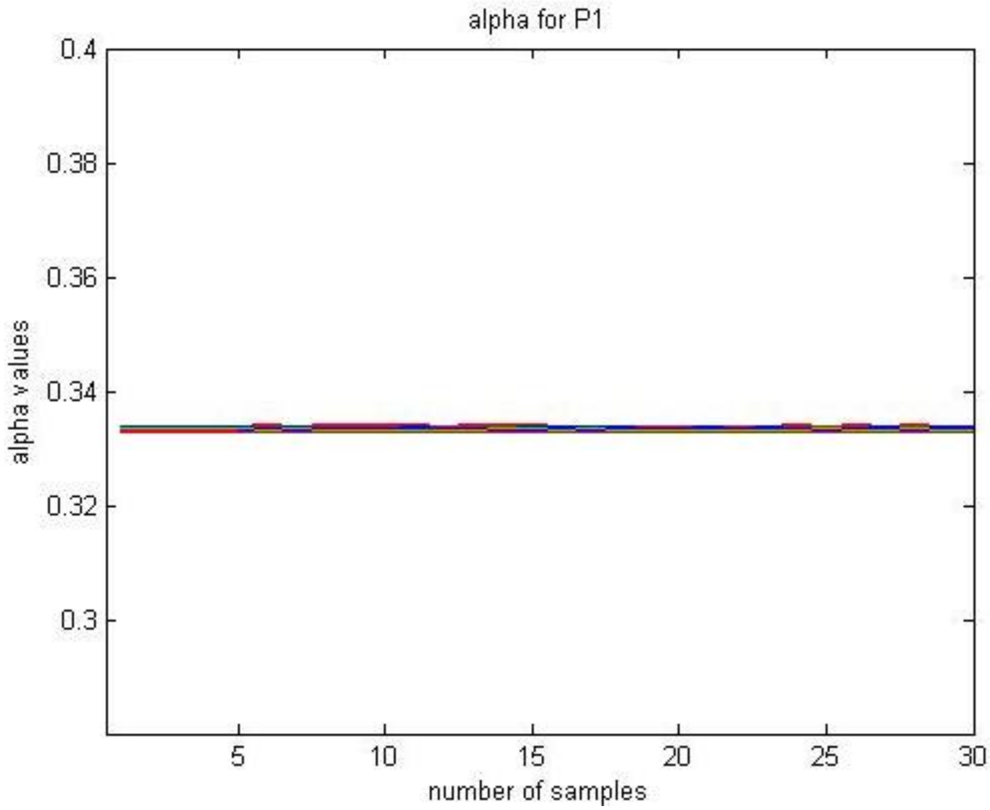

Fig. 5.13 – Alpha values for input chosen in P1

Next, it was necessary to ensure that the algorithm returned incorrect values of α when an incorrect $x(m)$ is chosen. The values of the F_1 matrix are kept the same. The input vertices which compose $x(m)$ are changed as seen in (5.18).

$$x(m) = \frac{1}{3}(x_1(m) + x_2(m) + x_5(m)) \tag{5.18}$$

The vector is now composed of values representative of the vertices of P_2. Though the weighting is still the same, the vertices provided cannot be controlled by the same controller as P_1. The resulting $\alpha_1, \alpha_2, and, \alpha_5$ are exactly as predicted. They do not form a convex combination with the polytopic variables, and thus do not make a convex set. Fig. 5.14 shows how sporadic these α values are.

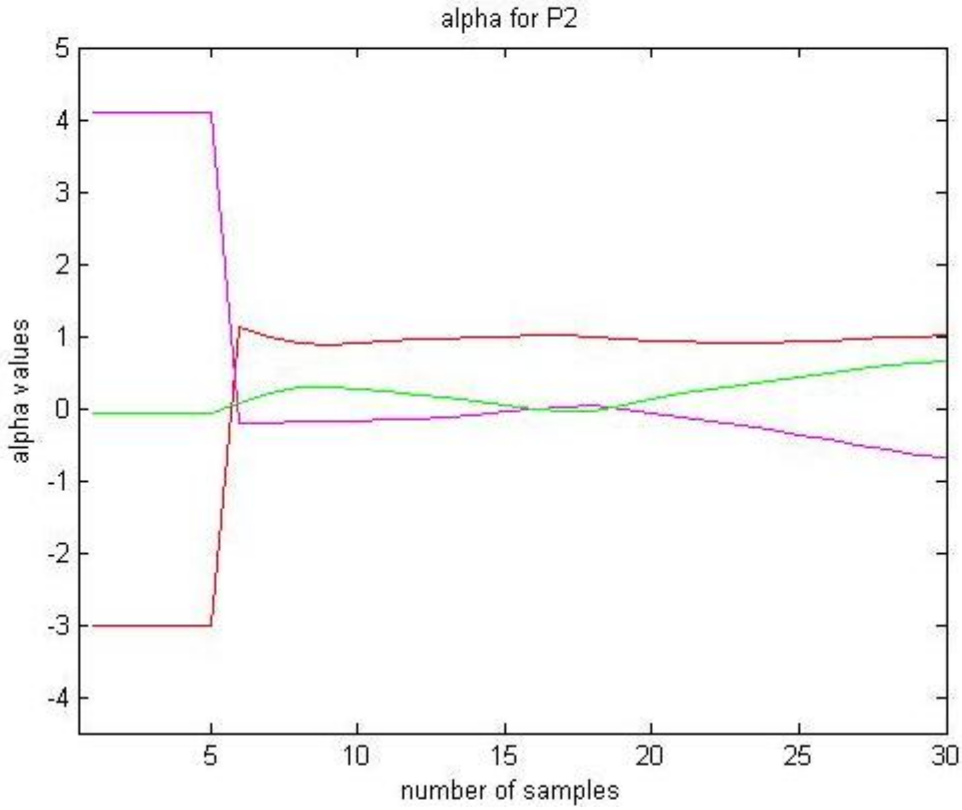

Fig. 5.14 – Alpha values for input chosen in P2

Additionally, when the controller, K_1, was applied to test scenario in P_1 it provided satisfactory damping as seen through the root locus plot in Fig. 5.15.

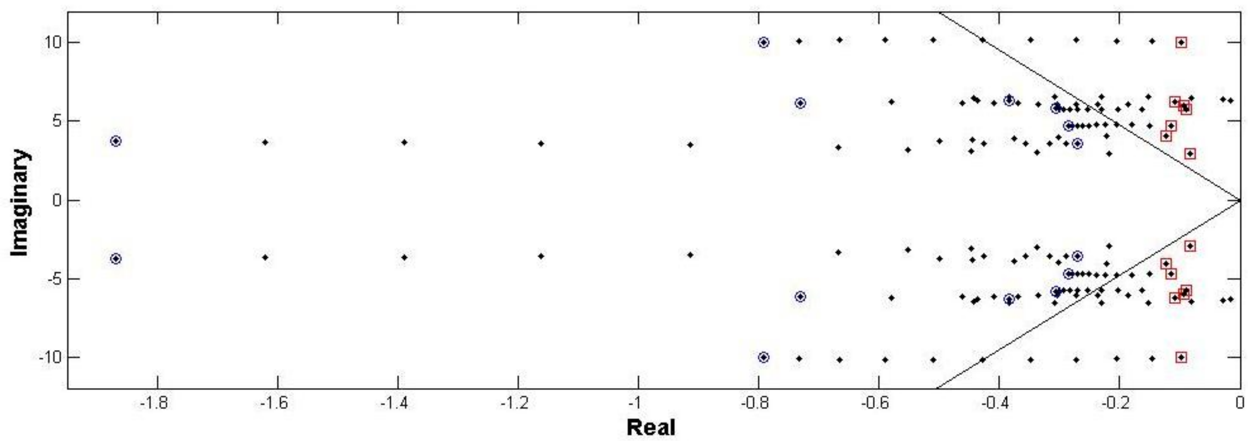

Fig. 5.15 – Damped eigenvalues of test input

Fig. 5.15 indicates that the control applied to the test scenario adequately damped the modes.

5.5 – Conclusions on Testing

The testing of this system showed positive results. The LMI controller worked well and provided a reasonable amount of damping to the inter-area modes. Some of the modes had less than 1% damping; therefore, improving that to 5% is satisfactory. This amount of damping is not what is actually desirable, but with one control in the system, it is acceptable. With more controls in the system, further damping could be achieved. When evaluating other inter-area modes in the system, it became obvious that another mode could be damped with an SVC potentially. The location of this mode was found by utilizing the same logic that was used in deciding correct the DC line placement.

It should be noted that the logic used in the DC line placement is flawed for larger systems. It does not provide the necessary amount of information needed about the controllability of a mode in large systems. [26] provides more information about using the Geometric Means of Controllability (GMC) to determine the location of Energy Storage Devices (ESDs). The ESDs were placed in a system model in the locations determined by the GMC. They demonstrated their ability to improve system stability.

This testing procedure is also considered successful because the adaptable control proved to indicate accurately whether an operating point was contained within a polytope by heuristically testing convexity. More rigorous proofs would be necessary as this technique can yield inaccurate results if there were an unforeseen condition that could not be detected in this manner.

Chapter 6 - Conclusion

The control techniques explored in this thesis offer a broad range of tools for tackling a very large and long standing problem: inter-area oscillations. The LMI polytopic formulation allows for many different and opposite constraints to be fulfilled while still finding a single sub-optimal controller. The way these control problems were synthesized is advantageous because it overcomes the problems associated with locally measured controllers by using WAMS as inputs to the controllers. After solving several polytopes for their individual control, the adaptive control algorithm is applied. It determines if the input signal to the algorithm can be classified as being inside the convex set created in any of the polytopes.

The various control devices also offer solutions for the problems at hand. Many of these FACTs based devices are becoming more popular, less expensive, and more common. Their popularity will continue because of these factors. Additionally, utilizing FACTs devices to increase stability has an economic and environmental component too. Using them is an economically sound way to increase stability, at least in the shorter term. Also, it is more environmentally conservative to utilize this technology than build more transmission lines [30]. It could also cost less money as discussed in Chapter 2.

Power system stability has been an issue since the beginning of the grid. As power demand continues to grow, the transmission system becomes more susceptible to failure. The relentless consumption of electricity threatens the livelihood of the system. Because electricity has become a necessity of life, it requires engineers to protect the integrity of the system. This is the point where we, as engineers, enter the picture. This thesis provides a small contribution towards the ultimate goal of power system stability. Even though this thesis develops an algorithm in a theoretical world, it may one day be developed into something which could be applied to a real network. Twenty years ago digital relays were considered inconsistent and impossible to implement, but one would find it difficult to locate a working electro-mechanical relay in a substation now.

6.1 – Future Scope of Work

Further work on this topic is extensive. This work can be used as a platform for many different problems. Several different areas for future work are described briefly in this section, though there are more to discover.

6.1.1 – Expand the number of vertices

In order to broaden the contingencies covered, more vertices can be added to the polytopic formation. If they are fairly similar, the control should be feasible and the regions will be expanded.

6.1.2 – Selective Modal Analysis (SMA)

This tool can be used to reduce the system size and complexity as detailed in [16, 26]. By applying it to a system and using a combined polytopic formulation, many more contingency cases could be covered.

6.1.3 – Integration of PSSs

In this thesis, the inputs from the PSSs were not considered in the control. This work could provide a more robust control if these inputs were included into the algorithm. However, for this to be a valid option, more system state reduction would be necessary.

6.1.4 – Physical Implementation

There are many constraints to take into consideration if this theory will ever be truly applied to a real power system. There are issues of redundancy of signal transfer similar to that in protection schemes. What signals in the system are so important that they should be redundant would need to be determined. There would need to be testing of the information signals as well. Testing would also need to indicate if the firing angles used in the DC implementation are correct. In power system protection, a relay can be removed from service for extensive testing. How can this system be checked if it cannot be removed? Additionally, if a mode were to occur, does the utility manager rely on the control algorithm to work without his or her input? The generally conservative nature of the power systems industry would indicate that an operator would see a mode and put the correct type of control into place. However, this could be adapted into a completely automated system.

References

[1] A. P. Sakis Meliopoulos, *Power System Modeling, Analysis and Control.* New York, Marcel Dekker 2004.

[2] B. Pal & B. Choudhuri, *Robust Control in Power Systems.*, New York: Springer, 2005, pp. 1–55.

[3] O. W. Hanson, *et al.,* Influence of Excitation and Speed Control Parameters in Stabilizing Intersystem Oscillations. Reprinted from *IEEE Trans Power App. Syst,* May 1968 in *Stability of Large Electric Power Systems,* R.T. Byerly, E.W. Kimbark, eds., IEEE Press, New York, 1974

[4] K. Mekki, N. HadjSaid, R. Feuillet, D. Georges, “Design of damping controllers using linear matrix inequalities techniques and distant signals to reduce control interactions,” *IEEE 2001 Power Industry Computer Applications Conference, 2001.*

[5] Y. Zhang and A. Bose, "Design of Wide-Area Damping Controllers for Interarea Oscillations," *IEEE Trans. Power Syst*, 2008.

[6] B. Chaudhuri, B. C. Pal, “Robust damping of multiple swing modes employing global stabilizing signals with a TCSC,” IEEE Trans. on Power Syst., Vol. 19, No. 1, pp. 499-506, Feb. 2004.

[7] A. F. Snyder, A. E. Mohammed, D. Georges, T. Margotin, N. Hadjsdid, and L. Mili, "A robust damping controller for power systems using linear matrix inequalities," in *Power Engineering Society 1999 Winter Meeting, IEEE*, 1999, pp. 519-524 vol.1.

[8] Saribulut L., TumayM.,EKERĐ.,Performance Analysis of Fuzzy Logic Based Unified Power Flow. Controller, International Journal of Electrical Power and Energy Systems Engineering, Vol: 2, Issue: 4, 2009, pp. 193-201.

[9] L'Abbate, A.; Migliavacca, G.; Häger U.: Rehtanz, C.; Rüberg, S.; Ferreira, H.; Fulli, G.; Purvins, A.; The role of FACTS and HVDC in the future pan-European transmission system development, 2010, 19-22 Oct 2010, ACDDC Conference, London (UK)

[10] J. Machowski, et al, Power System Dynamics and Stability, West Sussex, England: Wiley, 1997.

[11] C. Glover, *et al.*, *Power System Analysis and Design*, Toronto, Canada, Thomson, 2008, ch. 5, pp. 228-354.

[12] Chan-Ki Kim, *et al*., *HVDC Transmission,* John Wiley & Sons (Asia), 2009

[13] *Standard Handbook for Electrical Engineers*, New York: McGraw-Hill, 2006, pp. 15-1 – 15-35.

[14] Hui Ni, *et al.*, Power System Stability Agents Using Robust Wide Area Control , *IEEE Trans. Power Syst.*, vol. 17, no. 4, p.1123, Nov. 2002.

[15] G. J. Rogers, "The Application of Power System Stabilizers to a Multi-generator Plant", *IEEE Trans. Power Syst.*, Vol. 15, No. 1, pp. 350-355, Feb. 2000.

[16] Anamitra Pal, and James S. Thorp, "Co-ordinated control of inter-area oscillations using SMA and LMI", accepted for publication in IEEE PES Conference on Innovative Smart Grid Technologies

[17] G. Rogers, *Power System Oscillations*. Norwell, MA: Kluwer, 2000. OR

[18] P. Kundur, Power System Stability and Control, New York: McGraw-Hill, 1994.

[19] P. Kundur; M. Klein, G. J. Rogers, and M. S. Zywno, "Application of power system stabilizers for enhancement of overall system stability," Power Systems, IEEE Transactions on, Vol. 4, No. 2, pp. 614-626, 1989.

[20] S. Skogestad, and I. Postlethwaite, Multivariable Feedback Control, New York: Wiley, 2001.

[21] J. Rugh, Linear system theory (2nd ed.), Princeton, NJ: Prentice-Hall, Inc., 1996.

[22] M. Klein, G. J. Rogers, and P. Kundur, "A fundamental study of inter-area oscillations in power systems," *Power Systems, IEEE Transactions on*, Vol. 6, No. 3, pp. 914-921, Aug. 1991.

[23] D. N. Kosterev, W. Taylor, and W. A. Mittelstadt, "Model validation for the August 10, 1996 WSCC system outage," IEEE Trans. on Power Syst., Vol. 14, No. 3, pp. 967-979, Aug. 1999.

[24] A. Snyder, M. Alali, N. Hadjsaid, D. Georges, T. Margotin, and L. Mili, "A robust damping controller for power systems using linear matrix inequalities," in Proc.1999 Winter Meeting IEEE Power Eng. Soc., vol. 1, pp. 519–524

[25] R. Ranjan, P. Sauer, M. Pai, "Analytical formulation of small signal stability analysis of power system with nonlinear load models," in Sadhana., Springer Inidia, 1993, pp. 869-889.

[26] Anamitra Pal, "**Damping low frequency oscillations in the WECC**," *Final Project Report, Public Interest Energy Research (PIER) Program, TRP-08-06*, prepared for California Energy Commission by Virginia Polytechnic Institute and State University, Blacksburg, Virginia, Nov. 2011.

[27] P.L. So, *et al*., "Coordinated Control of TCSC and SVC for System Damping Enhancement*," International Journal of Control, Automation, and Systems*, vol. 3, no. 2 (special edition), pp. 322-333, June 2005.

[28] J. Ma, S. Garlapati, and J. Thorp, "Robust WAMS based control of inter area oscillations", *Electric Power Components and Systems*, Vol. 39, No. 9, pp. 850-862, May 2011.

[29] Chan-Ki Kim, *et al*., *HVDC Transmission,* John Wiley & Sons (Asia), 2009

[30] Woodford, D. A., *HVDC Transmission*, Manitoba HVDC Research Centre, Winnipeg, Manitoba,18 March 1998

[31] Boyd, S., Ghaoui, L. E., Feron, E. and Balakrishnan, V. (1994). *Linear Matrix Inequalities in System and Control Theory*, Studies in Applied Mathematics, SIAM.

[32] M. Chilali, P. Gahinet, and P. Apkarian, "Robust pole placement in LMI regions," *Automatic Control, IEEE Transactions on*, vol. 44, pp. 2257-2270, 1999.

[33] M. Chilali and P. Gahinet, "Hinfinity design with pole placement constraints: an LMI approach," *Automatic Control, IEEE Transactions on*, vol. 41, pp. 358-367, 1996.

[34] P. Gahinet, A. Nemirovski, A. J. Laub, and M. Chilali, *LMI Control Toolbox for use with MATLAB*, The Math Works, Inc., USA.

[35] A. Megretski, (2005). *Optimization Methods in Analysis and Design of Linearized Systems.* Available FTP: http://www-ma4.upc.edu/~carles/ioc17013/Optimization%20Methods%20in%20Analysis%20and%20Design%20of%20Linearized%20Systems.pdf

[36] A.M Cristobal , "Multiobjective Control: Linear Matrix Inequality Techniques and Genetic Algorithms Approach," Ph.D. dissertation, Dept. of Automatic Control and Systems Eng., The Univ. of Sheffield, Sheffield, UK, 2005.

[37] K Chang and W Chang, "Multi-objective control design for stochastic large-scale systems based on LMI approach and sliding mode control concept," Journal of Marine Science and Technology, vol. 16, no. 3, pp. 197-206, 2008.

[38] P. Dorato, Abdallah, C. T., Linear Quadratic Control: An Introduction, Malabar, FL: Krieger Publishing Company, 2000.

[39] RE Kalman, RS Busy, “New results in linear filtering and prediction theory” Trans. ASME Ser. D. (J. Basic Engr.) 83, 1961: 95-107.

[40] M. Bouhamida and M.A. Denai. “Robust stabilizer of electric power generator using Hinf with pole placement constraints.” *Journal of Electrical Engineering*, vol. 56, no. 7-8, pp.176-182, 2005.

[41] P. S. Rao and I. Sen, "Robust pole placement stabilizer design using linear matrix inequalities," *Power Systems, IEEE Transactions on,* vol. 15, pp. 313-319, 2000.

[42] C. Scherer, P. Gahinet, and M. Chilali, "Multiobjective output-feedback control via LMI optimization," *Automatic Control, IEEE Transactions on,* vol. 42, pp. 896-911, 1997.

[43] L. Zadeh, "Optimality and non-scalar-valued performance criteria," *Automatic Control, IEEE Transactions on,* vol. 8, pp. 59-60, 1963.

[44] A. Bensenouci and A. M. A. Ghany, "Mixed H2/Hinf with pole-placement design of robust LMI-based output feedback controllers for multi-area load frequency control," in *EUROCON, 2007. The International Conference on "Computer as a Tool"*, 2007, pp. 1561-1566.

[45] G.E. Franklin, J.D. Powell and A. Emami-Naeini. *Feedback Control of Dynamic Systems*, 5th ed. Upper Saddle River, NJ: Pearson Prentice Hall, 2006.

[46] C. W. Scherer, "Mixed H-2/H-Infinity Control. *Trends in Control, A European Perspective*,” I. A. Delft, The Netherlands, Springer-Verlag, pp. 173-216. , 1995.

[47] Alizadeh, F., Haeberly, J.-P. A., and Overton, M. L. (1998). Primal-dual interior-point methods for semidefinite programming: convergence rates, stability and numerical results. SIAM J. Optim., 8(3):746{768.

[48] D. Arzelier and D. Peaucelle, "An iterative method for mixed H2/Hinf synthesis via static output-feedback," in *Decision and Control, 2002, Proceedings of the 41st IEEE Conference on,* 2002, pp. 3464-3469 vol.3.

[49] M. Dettori and C. W. Scherer, "MIMO control design for a compact disc player with multiple norm specifications," *Control Systems Technology, IEEE Transactions on,* vol. 10, pp. 635-645, 2002.

[50] C. W. Scherer, "Multiobjective H2/Hinf control," *Automatic Control, IEEE Transactions on*, vol. 40, pp. 1054-1062, 1995. B

[51] P. P. Khargonekar and M. A. Rotea, "Mixed H2/Hinf control: a convex optimization approach," *Automatic Control, IEEE Transactions on*, vol. 36, pp. 824-837, 1991.

[52] J. F. Camino, J. W. Helton, and R. E. Skelton, "Solving matrix inequalities whose unknowns are matrices," *43rd IEEE Conference on Decision and Control, 2004, CDC*, Vol. 3, pp. 3160-3166, 2004.

[53] S. P. Boyd and L. Vandenberghe, *Convex optimization*. Cambridge, UK; New York: Cambridge University Press, 2004.

[54] M. Dean, (2010). Convex Analysis [Online]. Available: http://www.econ.brown.edu/fac/Mark_Dean/Maths_CA1_10.pdf

Appendix A

Appendix 1 provides the necessary information for a load flow for the base case of the test system.

This is the bus information for my test system. Bus types: 1 is slack, 2 is generator, 3 is load.

Bus Num	Voltage Mag (PU)	Voltage Angle (deg)	P Gen	Q Gen	P Load	Q Load	G Shunt	B Shunt	Bus Type	Q Gen Max	Q Gen Min	Voltage Rated (kV)	V Max	V Min
1	1	3.9	124	75	115	55	0	0	2	9999	-9999	13.8	1.05	0.93
2	1	29.6	130	65	80	30	0	0	2	9999	-9999	13.8	1.05	0.93
3	1	36.7	102	65	62	28	0	0	2	9999	-9999	13.8	1.1	0.9
4	1	0.7	110	40	40	15	0	0	2	9999	-9999	13.8	1.05	0.93
5	1.01	15.2	120	74	110	50	0	0	2	9999	-9999	13.8	1.05	0.93
6	1	0	-66.94	-2.63	30	12	0	0	1	0	0	13.8	1.05	0.93
7	1	65.8	47	25.82	10	4	0	0	2	9999	-9999	13.8	1.05	0.93
8	1	29.5	54	-53	60	22	0	0	2	9999	-9999	13.8	1.05	0.93
9	1	-2.3	0	0	25	15	0	0	3	0	0	132	1.05	0.93
10	0.99	-2.9	0	0	25	15	0	0	3	0	0	132	1.05	0.92
11	0.99	5.1	0	0	0	0	0	0	3	0	0	132	1.05	0.92
12	1	63.5	0	0	0	0	0	0	3	0	0	132	1.05	0.93
13	1	36.4	0	0	0	0	0	0	3	0	0	132	1.05	0.93
14	1	0	0	0	10.2	2.8	0	6	3	9999	-9999	13.8	1.05	0.9
15	1	0	0	0	-10.1	2.7	0	6	3	9999	-9999	13.8	1.05	0.9

The following is the line data.

To Bus	From Bus	Res (PU)	Reac (PU)	Line Charging (PU)	Tap Ratio	Phase Shift (deg)	Tap Max	Tap Min	Tap Size
1	2	0.0035	0.0001	0.22	0	0	0	0	0
1	5	0.003	0.003	0.2	0	0	0	0	0
1	6	0.0003	0.00282	0.02	0	0	0	0	0
1	6	0.0003	0.00285	0.09	0	0	0	0	0
2	13	0.0001	0.002	0.3	0	0	0	0	0
3	4	0.0001	0.0155	0.01	0	0	0	0	0
3	13	0.001	0.005	0	0	0	0	0	0
4	9	0.0001	0.0009	0.04	0	0	0	0	0
5	9	0.0064	0.00428	0.292	1.01	0	0	0	0
5	10	0.0019	0.0001	0.9	1	0	0	0	0
6	7	0.0019	0.0255	0.0952	0	0	0	0	0
6	11	0.0002	0.007	0	1.01	0	0	0	0
6	13	0.0004	0.02	0	0	0	0	0	0
7	12	0.0001	0.005	0	0	0	0	0	0
8	11	0.008	0.024	0.334	1.01	0	0	0	0
8	12	0.0085	0.008	0.7	0	0	0	0	0
8	13	0.0072	0.028	0.7	0	0	0	0	0
9	10	0	0.029	0	1	0	0	0	0
12	13	0.003	0.025	0	0	0	0	0	0
4	14	0	0.007	0	0	0	1.05	0.95	0.005
8	15	0	0.007	0	0	0	1.05	0.95	0.005

The following is information on the generators.

- x_l is the leakage reactance
- r_a is the resistance
- x_d' is the d-axis transient reactance (pu)
- x_q' is the q-axis transient reactance (pu)
- H is the generator inertia
- d_0 is the damping coefficient

Machine #	Bus #	Base MVA	x_l	r_a	x_d'	x_q'	H	d_0
1	1	5500	0.05	0	0.32	0.3	8.8	3.5
2	2	12000	0.05	0	0.25	0.25	9.2	3.5
3	3	16000	0.05	0	0.3	0.3	8	3.5
4	4	14000	0.05	0	0.32	0.32	9.6	2
5	5	9500	0.05	0	0.29	0.29	9.8	3.5
6	6	16000	0.05	0	0.15	0.15	10	2
7	7	5200	0.05	0	0.3	0.3	6.6	2
8	8	8000	0.05	0	0.6	0.6	6	4.5

Appendix B

The list that follows includes the programs which were developed for this thesis.

The inputs to this program “Postprocessing” are the outputs of running svm_mgen.m in the PSTV3 suite. They are the state matrices. This program just organizes the information such that it can be used in the Robust Control Toolbox in a more intuitive way.

```
%%%%%%%%%%%%%%%%%%%%%%%%%%%%%%%%%%%%%%%%%%%%%%%%%%%%
%                                                        %
% Program Name: Postprocessing                         %
%                                                      %
% Description: Organizes the matrices developed by PSTV3 into inputs for     %
% LMI control.                                          %
%                                                      %
% Author: Katelynn A. Vance                             %
%        Virginia Tech                                  %
%                                                      %
% Last Modified: 12/05/2011                             %
%                                                      %
%%%%%%%%%%%%%%%%%%%%%%%%%%%%%%%%%%%%%%%%%%%%%%%%%%%%

n = size(a_mat)*[1 0]';    % n = Size of System (with control as
                       % determined by PSTV3)
c = 4;                    % Number of controls as determined with PSTV3
rc = n - c;               % Number of controls we actually have available
                       % to model in the system. 1 in this case.
A = 0*eye(n);

r1 = find(mac_state(:,2)==1); % Gives states with rotor angle (ang_idx)
r2 = find(mac_state(:,2)==2); % Gives states with frequency (spd_idx)

r = [r1' r2'];

%%%%%%%% RAW CONTROLS --- matrices before they have been reduced
%%%%%%%%%%

A(1:n,1:n) = a_mat(r,r);    % Initialize A matrix

BB = 0*ones(n,c);          % Initialize B matrix
% Used for control of DC Lines
BB(:,1:2)=b_lmod(r,1:2);
BB(:,3:4)=b_rlmod(r,1:2);
```

```
C1S = c_ang(1,r);          % Necessary for the H_inf optimization
C2S = c_spd(1:7,r);        % Necessary for the H_2 optimization


% No D matrix was given in PSTV3, but one is needed for LMI control. It is
% added below

% Transformation vector used to create 1 control out of 4 variables
T = [ 1 -1 .3 .3];      % Reduction factor (4 to 1)
nc = size(T)*[1 0]';    % Number of reduced controls (here it is 1)


%%%%%%%% SYSTEM REDUCTION AND FORMULATION %%%%%%%%%
% A Matrix
An(1:rc,1:rc) = A(1:rc,1:rc);
An(1:rc,rc+1:rc+nc) = A(1:rc,rc+1:rc+c)*gamma';
An(rc+1:rc+nc,1:rc) = gamma*A(rc+1:rc+nc,1:rc);
An(rc+1:rc+nc,rc+1:rc+nc) = gamma*A(rc+1:rc+nc,rc+1:rc+nc)*gamma';
AA = An;

% B Matrix
Bnn = T*BB(rc+1:nn,1:nc)*T';
Bn = [ 0*ones(nc,rc) Bnn ]';
BB = [ Bn Bn ];

% C Matrix
C1 = C1S(:,1:rc+nc);
C2 = C2S(1:7,1:rc+nc);
CC = [ C1 ; C2 ];

% D Matrix
DD = 0*ones(8,nc*2);
DD(1,1) = 1;           % Contains 1 for D12 in Hinf (used for disturbance)
DD(2,2) = eye(nc);     % Contains 1 for D22 in H2 problem (used for input)
% Note, D21 = 0 and D12 = 0. D12 is not needed, but if it were a number,
% the robust control toolkit would still solve the LMI. If D21~=0, the
% program will not run


% Creation and storage of LTI System
S0 = ltisys(AA,BB,CC,DD,eye(rc+nc));
save numS0_BASE_8gensys_nov S0_nov
```

```
% Creation and storage of A matrix
A_test0 = AA(1:14,1:14);
save info_Atest0 A_test0

% Creation and storage of frequency
freq0 = freq;
save info_freq0 freq0;

% Creation and storage of delta
mac_ang0 = mac_ang;
save info_mac_ang0 mac_ang0;
```

The following program shows how the root locus plots were created.

```
%%%%%%%%%%%%%%%%%%%%%%%%%%%%%%%%%%%%%%%%%%%%%%%%%%%%%%%%%%%%%%%%
%                                                              %
% Program Name: Root Locus Information                         %
%                                                              %
% Description: Organizes the matrices developed by PSTV3 into inputs for %
%              LMI control.                                    %
%                                                              %
% Author: Katelynn A. Vance                                    %
%         Virginia Tech                                        %
%                                                              %
% Last Modified: 12/05/2011                                    %
%                                                              %
%%%%%%%%%%%%%%%%%%%%%%%%%%%%%%%%%%%%%%%%%%%%%%%%%%%%%%%%%%%%%%%%


%%%%%%%%%%%%%%%% ROOT LOCUS FOR S with K %%%%%%%%%%%%%%%

A = S(1:15,1:15);
B = S(1:15,17);
plot(eig(A),'rs')
hold on

% Iterates so you can see how the poles are moving towards the left

for i = 1:11
    g = .1*(i-1);
    plot(eig(A + g*B*K),'k.')
end
plot(eig(A+g*B*K),'bo')
axis([-2.2 0 -12 12])
x=[-9:1:0];
plot(x,-x/tan(.042),'k')
plot(x,x/tan(.042),'k')
title('Root Locus Plot for S with K')
xlabel('Real')
ylabel('Imaginary')
```

This is the formulation of the polytopic model. It includes the pole placement region and weighting for the norm of the H_2/H_∞ problem.

```
%%%%%%%%%%%%%%%%%%%%%%%%%%%%%%%%%%%%%%%%%%%%%%%%%%%%%%%%
%                                                  %
% Program Name: Simple PP                           %
%                                                  %
% Description: Creates Polytope and runs LMI synthesis      %
%                                                  %
% Author: Katelynn A. Vance                          %
%        Virginia Tech                              %
%                                                  %
% Last Modified: 12/05/2011                         %
%                                                  %
%%%%%%%%%%%%%%%%%%%%%%%%%%%%%%%%%%%%%%%%%%%%%%%%%%%%%%%%


% Import the state space systems created in postpro %
load numS0_BASE_8gensys_nov
load numS1_lineOUT1_8gensys_nov
load numS2_loadchange2_8gensys_nov
load numS3_lineOUT3_8gensys_nov
load numS4_loadchange4_8gensys_nov

%polytopic model of the plant (choose one to run)
Pols=psys([S0_nov, S1_nov, S2_nov, S3_nov, S4_nov]);    %All 5 Cases
%Pols=psys([S0_nov, S2_nov, S3_nov]);              %POLYTOPE 1
%Pols=psys([S0_nov, S1_nov, S4_nov]);              %POLYTOPE 2

% Create the Pole Placement region with 5% Damping
region=[0 + 2.0000i     0        0.9990       -0.039
     0            0        0.039        0.9990  ];

%size of d22 matrix (8 machines - 1 for slack)
r = [7 1];

% obj = [0 0 .5 .5] which provides the weighting of H2/Hinf trade off
obj = [0 0 .5 .5];


% PROBLEM SOLVED BY MATLAB:
[gopt,h2opt,K,Pcl]=msfsyn(Pols, r, [0 0 .5 .5], region);
% Returns:
  %gopt = guaranteed Hinf performance
  %h2opt = guaranteed H2 performance
  %K = gain matrix
```

```
    %Pcl = closed loop system


% Save K matrix for use in plotting the root locus plots
K1 = K;
save k1_nov K1
```

The following is the control algorithm. It is just applied to the small case given in Chapter 5.

```
%%%%%%%%%%%%%%%%%%%%%%%%%%%%%%%%%%%%%%%%%%%%%%%%
%                                              %
%  ALGORTHIM: Adaptive Control Algorithm       %
%                                              %
%  Description: Finds which K to apply to the input vector %
%                                            %
%                                             %
%                                              %
%   AUTHOR: Katelynn A. Vance                  %
%           Virginia Tech                      %
%                                              %
%   LAST MODIFIED:  12/05/11                   %
%                                              %
%%%%%%%%%%%%%%%%%%%%%%%%%%%%%%%%%%%%%%%%%%%%%%%%

%%% How to choose which control to use based on which A matrix is given

%STEP 1:
%%% Load A matrices, frequencies, and machine angles from cases

load info_Atest0_nov
load info_Atest1_nov
load info_Atest2_nov
load info_Atest3_nov
load info_Atest4_nov

load info_freq0_nov;
load info_freq1_nov;
load info_freq2_nov;
load info_freq3_nov;
load info_freq4_nov;

load info_mac_ang0_nov;
load info_mac_ang1_nov;
load info_mac_ang2_nov;
```

```
load info_mac_ang3_nov;
load info_mac_ang4_nov;



%STEP 2:
%%% Find phi from A to do the transformations necessary, use c2d
%[sysd,G] = c2d(sys,Ts,method) discretizes the continuous-time LTI model
%sys using zero-order hold on the inputs and a sample time of Ts seconds


% This is done for each A matrix of the polytope vertices
b = length(A_test0_nov);
B = zeros(b,1);     %it gives me the error "too few arguments" if I don't
                    %have a B element

[PHI0,G] = c2d(A_test0_nov,B,1/30);
[PHI1,G] = c2d(A_test1_nov,B,1/30);
[PHI2,G] = c2d(A_test2_nov,B,1/30);
[PHI3,G] = c2d(A_test3_nov,B,1/30);
[PHI4,G] = c2d(A_test4_nov,B,1/30);

%%%%%%% We need all of the frequencies (since it is a 14x1 vector where
%%%%%%% each of them repeat, we just want the odd ones). The resulting
%%%%%%% vectors for f0, etc will be 7x1. A similar process is done for the
%%%%%%% machine angles. After adding the two together, [delta0; f0] = 14x1.
%%%%%%% These vectors must be in this order because the A matrices which
%%%%%%% they are being compared to have correspond to states organized like
%%%%%%% this.

r = [1;3;5;7;9;11;13];
f0 = freq0_nov(r,1);
f1 = freq1_nov(r,1);
f2 = freq2_nov(r,1);
f3 = freq3_nov(r,1);
f4 = freq4_nov(r,1);

s = [1;2;3;4;5;7;8];
delta0 = mac_ang0_nov(s,1);
delta1 = mac_ang1_nov(s,1);
delta2 = mac_ang2_nov(s,1);
delta3 = mac_ang3_nov(s,1);
delta4 = mac_ang4_nov(s,1);


z = 0:.0333:1;      % x changes every 30th of a second
```

```
n = 30;             % get 30 points worth of data
states = 14;        % # of states in the system
S = z*states;       % number of values once you scan through the windows

%%% Now we have all of the x values from the delta/omega values to start
%%% solving for:
%%% x(n)= PHI*x(n-1)*alpha where...
   % PHI is 14x14
   % x(n-1) must be 14x3
   % alpha is 3x1
   % x(n) = 14x1
% Note: these are the dimentions for each discrete time period.

xx0 = [delta0; f0];
x0 =  xx0(:,ones(n,1)); % state variable 0

xx1 = [delta1; f1];
x1 =  xx1(:,ones(n,1)); % state variable 1

xx2 = [delta2; f2];
x2 =  xx2(:,ones(n,1)); % state variable 2

xx3 = [delta3; f3];
x3 =  xx3(:,ones(n,1)); % state variable 3

xx4 = [delta4; f4];
x4 =  xx4(:,ones(n,1)); % state variable 4

%%%%%%%::::EQUATION::: x(n) = PHI*x(n-1)
%%% x(n) = (PHI0*x0(n-1)+PHI1*x1(n-1)+ PHI2*x(n-1))*alpha
%%% F is the PHI*x(n-1) in completion (it is 14x3)
%%% NOTE:: these dimensions are all for just one value of n, they will
%%% scale by a factor of 14*n


%% Begin Algorithm %%
alpha(1:3,n) = 0; %initialize alpha for 30 inputs

for a = 1:n
        %%% first 5 found non recursively
        if  a <= 5

            x0(:,a) = PHI0*x0(:,a);
            % Need to reorder the x0 values because right now, it is a
            % 14x30 matrix, but it actually needs to be a singular
            % vector 420x1. Where 420=14*30. Use a change of variables.
```

```
    z0(a*states-states+1:a*states,1) = 0;
    z0(a*states-states+1:a*states,1) = x0(:,a);
    % The values of z0... are what make up each column of the F
    % matrix.
    % Use a*states so that for each time a changes, another set
    % of rows the length of the states is added onto the
    % vector.

    x1(:,a) = PHI1*x1(:,a);
    z1(a*states-states+1:a*states,1) = 0;
    z1(a*states-states+1:a*states,1) = x1(:,a);

    x2(:,a) = PHI2*x2(:,a);
    z2(a*states-states+1:a*states,1) = 0;
    z2(a*states-states+1:a*states,1) = x2(:,a);

    x3(:,a) = PHI2*x3(:,a);
    z3(a*states-states+1:a*states,1) = 0;
    z3(a*states-states+1:a*states,1) = x3(:,a);

    x4(:,a) = PHI1*x4(:,a);
    z4(a*states-states+1:a*states,1) = 0;
    z4(a*states-states+1:a*states,1) = x4(:,a);

    % Now, calulate F1 = PHI*x(n-1) of dimension 14x3.
    F1 = [z0 z2 z3];
    % Use this to now solve the pseudo-inverse in this problem
    alpha1(1:3,a) = inv(F1(a*states-states+1:a*states,:)'...
      *F1(a*states-states+1:a*states,:))*...
      (F1(a*states-states+1:a*states,:)')*1/3*(x0(:,a)+x2(:,a)+x3(:,a));

     F = [z0 z1 z4];
     alpha(1:3,a) = inv(F(a*states-states+1:a*states,:)'...
        *F(a*states-states+1:a*states,:))*...
        (F(a*states-states+1:a*states,:)')*1/3*(x0(:,a)+x1(:,a)+x4(:,a));



else
    % Now, the algorithm is solved recursively

    x0(:,a) = PHI0*x0(:,a-1);
    z0(a*states-states+1:a*states,1) = 0;
    z0(a*states-states+1:a*states,1) = x0(:,a);

    x1(:,a) = PHI1*x1(:,a-1);
```

```
        z1(a*states-states+1:a*states,1) = 0;
        z1(a*states-states+1:a*states,1) = x1(:,a);

        x2(:,a) = PHI2*x2(:,a-1);
        z2(a*states-states+1:a*states,1) = 0;
        z2(a*states-states+1:a*states,1) = x2(:,a);

        x3(:,a) = PHI2*x3(:,a-1);
        z3(a*states-states+1:a*states,1) = 0;
        z3(a*states-states+1:a*states,1) = x3(:,a);

        x4(:,a) = PHI1*x4(:,a-1);
        z4(a*states-states+1:a*states,1) = 0;
        z4(a*states-states+1:a*states,1) = x4(:,a);

        F1 = [z0 z2 z3];
        alpha1(1:3,a) = inv(F1(a*states-states+1:a*states,:)'...
            *F1(a*states-states+1:a*states,:))*...
            (F1(a*states-states+1:a*states,:)')*1/3*(x0(:,a)+x2(:,a)+x3(:,a));

        F = [z0 z1 z4];
        alpha(1:3,a) = inv(F(a*states-states+1:a*states,:)'...
            *F(a*states-states+1:a*states,:))*...
            (F(a*states-states+1:a*states,:)')*1/3*(x0(:,a)+x2(:,a)+x3(:,a));

    end

end

plot(1:n,alpha1(1,:),'Color','red','LineWidth',3)
hold on
plot(1:n,alpha1(2,:),'Color','blue','LineWidth',2)
plot(1:n,alpha1(3,:),'Color','green')
title('alpha for P1')
xlabel('number of samples')
ylabel('alpha values')
axis([.5 30 .28 .40])
figure
plot(1:n,alpha(1,:),'Color','red')
hold on
plot(1:n,alpha(2,:),'Color','magenta')
plot(1:n,alpha(3,:),'Color','green')
title('alpha for P2')
xlabel('number of samples')
ylabel('alpha values')
axis([.5 30 -4.5 5]
```

Appendix C

This includes the letter which allows me to cite the research done by Arturo Cristobal. This is seen in Fig. A3.1.

Kate Vance to am664 — show details Dec 14 (4 days ago) — Reply

Hello,

I am in the direct-PhD program at Virginia Tech. On my way to my PhD, I decided to write a MS Thesis as well. I am working in the area of power systems, but have applied LMI theory to my control problem. Your dissertation relates to my thesis topic, and I wanted to know if you would be so kind as to allow me to use some of your information provided in your dissertation. I attached the file where your work has been mentioned. I currently have it as [CRISTOBAL] so it would be easy for you to see where I had cited you. However, when it is completed, I will properly cite everything using the IEEE style. I look forward to your response, and please let me know if you have any questions.

Thank you,
Kate Vance

Chapter 3.docx
104K View Download

Reply Forward

arturo molina-cristobal am664@cam.ac.uk to me — show details Dec 16 (2 days ago) — Reply

Dear Kate,

Thank you for your enquire. Apologies for the delay, I was traveling for holidays and I didn't see your email until today. Regarding my PhD thesis, please find the attached file.

I am interested in Power Systems, as you can see from my publications. I found interesting your research area, please let me know when your MS dissertation is ready and I would like to have a copy.

I tried to open you word document (Chpater 3 .docx), however my word processor cannot open the file, would you please send me another version or a PDF copy.

Best regards,

Arturo

- Show quoted text -

PhDthesis_molina-cristobal.pdf
1160K View Download

Reply Forward

Fig. C.1 – Letter of permission